The Chemistry behind Catechol-Based Adhesion

J. Saiz-Poseu,* J. Mancebo-Aracil, F. Nador, F. Busqué, D. Ruiz-Molina*

Abstract: The wet adhesion of some marine organisms to almost any kind of surface has aroused increasing interest over recent decades. Numerous fundamental studies have been performed to understand the scientific basis of this behaviour, where catechols have been found to play a key role. Several novel bioinspired adhesives and coatings with value-added performances have been developed by taking advantage of the knowledge gained from these studies. Excellent reviews of this issue have been published due to the large amount of interest and generated literature. Nevertheless, no detailed compilation exclusively focused on the complex inner workings of these materials exists. Thus, the aim of this work is to review recent investigations that elucidate the origin of the strong and versatile adsorption capacities of the catechol moiety and the effects of extrinsic factors playing important roles in the overall adhesion process, such as pH, solvent and the presence of metal ions. In other words, it is our aim to review in detail the chemistry behind the astonishing properties of natural and synthetic catechol-based adhesive materials.

1. Introduction

Many marine organisms have developed natural mechanisms to firmly attach to underwater surfaces. Their objective is to prevent their movement by currents and tides so they can perform basic vital functions such as feeding and reproduction. Representative examples of organisms with these mechanisms are sandcastle worms,[1] barnacles [2,3] and mussels,[4,5,6,7] which mostly base their adhesion on the secretion of specialized proteins. For instance, mussels use natural holdfasts called byssus to attach onto rocks and almost any kind of surface they find underwater. These anchoring elements are composed of several proteins that are secreted during the adhesion process.[1,7] A detailed study of these mussel foot proteins (mfps) showed that their most representative feature is an atypically high concentration of the catecholic amino acid 3,4-dihydroxy-L-phenylalanine (DOPA), which is obtained by the post-translational enzymatic hydroxylation of tyrosine.[8] Such a high concentration is especially relevant in mfp-3 and mfp-5 (21%[9] and 27%[10] DOPA content, respectively, for *Mytilus edulis*), key components of a plaque that contacts surfaces during adhesion. DOPA was thus suggested to play a key role on this process, which was experimentally confirmed in subsequent works.[11,12]

Currently, a wide consensus among the scientific community considers catechol as the origin of the astonishing adhesion capacities of mussels and other marine wildlife. This discovery, besides its raising of inherent interest, also represents a starting point in the development of novel synthetic wet adhesives and coatings, a scientific and technical challenge. This discovery is especially relevant in areas such as biomedicine, where high adhesion capacities in aqueous environments are at a premium.[13,14,15,16,17] The need to adhere different body parts through suturing and wound sealing is a representative example.[18,19,20,21] However, catechols also represent a quite easy, reliable and effective way to functionalize surfaces. The paradigm is the *in situ* polymerization of dopamine under mild basic conditions, which is broadly used by several different groups worldwide. Such polymerization generates a strongly adherent coating (primer) of polydopamine, which can be later functionalized with the aim of transferring given properties (e.g., hydrophobicity/hydrophilicity or bioactivity) to the substrate.[22]

According to the prospects previously described, the number of publications reporting catechol-based adhesives and coatings has grown over the years. Most of them have been compiled in excellent reviews focusing on the material characteristics and applications.[23] An updated version gathering novel examples is thus outside the scope of the present work. In contrast, at the time of writing this manuscript, detailed reviews analysing and correlating the actors affecting the chemistry behind the adhesion of these materials were lacking; these materials usually involve far more than catechols and related factors such as their organization[24] and structuring at the nanoscale.[25] With this aim, we have classified this revision to cover two main areas: I) a description and understanding of the different interactions and bonds that catechols establish with surfaces in the anchoring step, i.e., the adsorption phenomena and II) factors that may influence the effectiveness of the overall adhesion (i.e., adsorption and bulk cohesion) such as catechol content, the presence of other species in the material backbone, pH, redox activity and the presence of ions in the environment. Finally, concluding remarks will gather the different actors modulating the effectiveness of these systems while highlighting future approaches to improving catechol-based adhesive materials and coatings.

[*] Dr. J. Saiz-Poseu, Dr. D. Ruiz-Molina
Catalan Institute of Nanoscience and Nanotechnology (ICN2), CSIC and BIST,
Campus UAB, Bellaterra, 08193 Barcelona, Spain
E-mail: javier.saiz@icn2.cat
dani.ruiz@icn2.cat

Dr. J. Mancebo-Aracil, Dr. F. Nador
Instituto de Química del Sur-INQUISUR (UNS-CONICET)
Universidad Nacional del Sur
Av. Alem 1253, 8000 Bahía Blanca, Buenos Aires (Argentina)

Dr. F. Busqué
Dpto. de Química (Unidad Química Orgánica)
Universidad Autónoma de Barcelona
Edificio C - Facultad de Ciencias, 08193 Cerdanyola del Vallès, Barcelona (Spain)

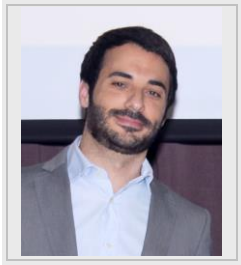

Javier Saiz-Poseu graduated in chemistry (2006) and received his PhD (2011) from the Universidad Autónoma de Barcelona. Co-directed by Félix Busqué and Daniel Ruiz-Molina, his work focused on the synthesis, characterization and macro/nanoscale application of catechol-based materials. After expanding the scope of these studies as a postdoctoral fellow, he is currently developing his career at the ICN2.

Daniel Ruiz-Molina earned his PhD on dendrimers, and after a postdoctoral position at UC San Diego working on switchable molecular materials, he secured a permanent position at the CSIC. More recently, he moved to the ICN2, where he is leading the Nanosfun group. His main research areas are the fabrication of biomimetic hybrid colloids and surfaces, encapsulation, nanoscale coordination polymers and smart optical materials

2. The nature of the catechol-surface interaction

Although very simple in its structure, composed of only a benzene ring bearing two neighbouring hydroxyl groups, catechol effectively interacts with almost any kind of surface. The secret to such a high versatility is associated with an exceptional surface adaptation ability: depending on the substrate nature, catechols can be adsorbed by means of different chemical interactions (Figure 1), ranging from weak dispersion forces to covalent bonds, which are discussed next.

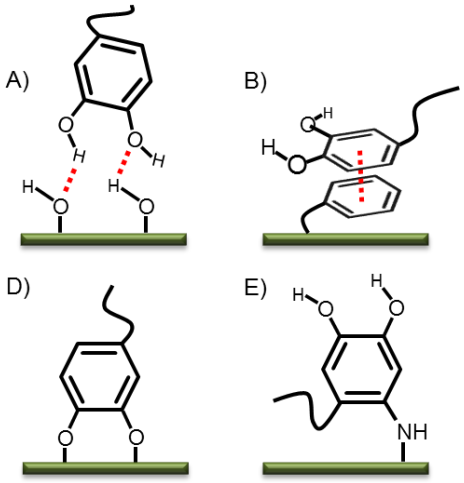

Figure 1. Schematic representation of the four main catechol-surface interactions described in this section: A) hydrogen bonding, B) π-π stacking, C) coordination and E) an example of covalent bonding with surface amines (via Michael-type addition).

2.1. Non-covalent interactions

2.1.1. Hydrogen bonding

Catechol groups have a strong affinity for hydrophilic surfaces thanks to their capacity to establish hydrogen bonds. How these interactions can be effective in an aqueous environment with a large excess of competing water molecules is unclear. To answer this question, researchers performed theoretical studies. Density functional theory (DFT) calculations analysed the energy balance for the interaction of pyrocatechol and water on α-cristobalite (001) and β-cristobalite (111).[26] These two hydroxylated silica surfaces were selected because of their similarity to underwater amorphous silica, where surface silicon atoms rapidly react with water to form silanols. The main results from this work were that I) pyrocatechol showed a higher affinity (14.15 and 11.65 kcal/mol for the (001) and (111) surfaces, respectively) than water molecules (1.98 and 0.57 kcal/mol) for both surfaces, II) the underlying lattice noticeably affects the adsorption process (pyrocatechol can establish four hydrogen bonds with the (001) lattice but only three with the (111) surface), and III) independently of the surface, catechols prefer to stand upright, i.e., nearly perpendicular to the surface plane, rather than lay flat. Taking into account this geometry and an average energy of approximately 3.7 kcal/mol per bond, it is feasible to consider hydrogen bonding (typically between 2.4-6.2 kcal/mol)[27] the most important interaction with amorphous wet silica surfaces. Interrelated calculations[28] and *ab initio* molecular dynamic (MD) simulations performed by Ganz et al.[29] also supported these results. The authors demonstrated that pyrocatechol displaces preadsorbed water molecules from the substrate by competitive hydrogen bonds and the help of dispersion forces from the phenylene ring.[29,30] Finally, both DFT and MD calculations noted the torsion capacity of the hydroxyl bonds as the origin of the enhanced versatility of catechols to effectively establish hydrogen bonds with different underlying lattices since they can freely rotate with respect to the phenylene ring to find an optimal adsorption geometry.[26,29]

In addition to theoretical approaches, experimental methods also confirmed the role of hydrogen bonding in the interaction of catechols with polar substrates. For instance, Israelachvili et al.[4] used an atomic force microscope (AFM) and a surface force apparatus (SFA) for studying the adhesive properties of two mfps (mfp-1 and mfp-3) from *M. edulis* on a poorly adherent mica substrate at the microscale. At a slightly acidic pH, AFM experiments confirmed the fast adhesion of mfp-1 to this aluminosilicate, whereas SFA evidenced two different roles: mfp-1 behaved as a protective coating, and mfp-3 was the real gluing agent (Figure 2). Although both proteins have similar DOPA content, the smaller size of the latter favours diffusion into the gaps of the substrate, allowing mfp-3 to form more binding sites because of its higher mobility and flexibility. This example showed how the presence of DOPA, though necessary, is not enough for ensuring effective gluing. Regarding the nature of the interactions between these proteins and the mica substrate, the authors concluded that the energy values and the reversibility of the process were indicative of non-covalent interactions, probably hydrogen bonding, though electrostatic forces could not be excluded.

Waite et al.[31] determined the adhesion capacity of mfp-1 to amorphous titania and mica surfaces with an SFA. This protein adhered strongly and reversibly to both substrates at a slightly acidic pH in a hydrated environment, with the adhesion strength of TiO_2 being roughly double that of mica. The reasons for this difference are I) the cumulative contribution of coordination and hydrogen bonds in the case of TiO_2[32,33,34] and II) the surface roughness (0.8 nm *vs.* 0.2 nm for TiO_2 and mica, respectively)

conditioning the number of effective bonding sites and thus the adhesion.[35, 36, 37] The same group also studied the role of catechols in the TiO_2 and hydroxyapatite adsorption of a peptide whose isoelectric point and hydrophobic characteristics mimicked those of mfp-3.[25] The adsorption was followed by a crystal microbalance with dissipation (QCM-D), and the results demonstrated that the presence of the catecholic amino acid DOPA accelerates the kinetics of the peptide adsorption on the hydroxyapatite surface.

Catecholic peptides exhibited longer binding lifetimes than the analogous tyrosine model thanks to bidentate hydrogen bonding capacity, which contributes a stronger interaction to displace water molecules from the surface.[25] The inability of the tyrosine-based peptide to remove surface moisture was demonstrated by attenuated total reflection infrared (ATR-IR) spectroscopy with a flow cell set-up. The broad and positive intensity of the *v*OH mode, assigned to interfacial water molecules at the hydroxyapatite, remained with time. These molecules would lead to weak hydrogen bond-based adsorption. In contrast, the intensity of the 4000 and 2500 cm^{-1} spectral regions of the DOPA-containing peptide decreased with time, indicating the removal of liquid-like interfacial water molecules. The same authors stressed the relevance to adhesion of other contributing forces such as cation-π interactions between the aromatic ring of DOPA/Tyr residues and Ca(II) from hydroxyapatite.

The importance of hydrogen bonding was also evaluated studying the adhesion capacity of DOPA-containing mfp-3 at different pH values.[38] By means of an SFA, Waite et al. showed that the adhesion was enhanced at an acidic pH value (3), where the prevalent state is the catechol form. In this case, the distance between substrate oxygen atoms (approximately 0.28 nm) perfectly matches the distance between the hydroxyl groups of the DOPA moiety (approximately 0.29 nm). This relation together with the previously mentioned torsion adaptability of the hydroxyl groups to the underlying surface lattice[26,39] definitely favours the formation of bidentate hydrogen bonds. When the pH is increased to 5 or oxidizing agents are added, the quinone form prevails over the catechol. At this point, the adhesion decreased by more than 60%, confirming the importance of hydrogen bonding in the adsorption mechanism. This fact was also supported by Robertson et al.,[40] who compared the adsorption properties of different catecholic and non-catecholic materials. A comparison of pyrocatechol and 3-hydroxytyramine with a mono-hydroxylated phenol showed that the catechol-bearing molecules adsorbed more strongly (approximately three orders of magnitude more strongly). The authors also suggested that the main mechanism is a cooperative binding through divalent hydrogen bonds on the hydroxyapatite crystal edges (occupancy previously reported for analogous experiments on alumina),[41] though additional contributions from electrostatic and aromatic interactions could not be discarded. In this sense, the authors noted a feasible close packing of the catechols within the monolayer favoured by an almost vertical position of the molecules. This orientation would allow a cooperative interaction between aromatic rings, thus enhancing the rate and energy of the adsorption by pulling other catechol groups from solution into the monolayer.[40]

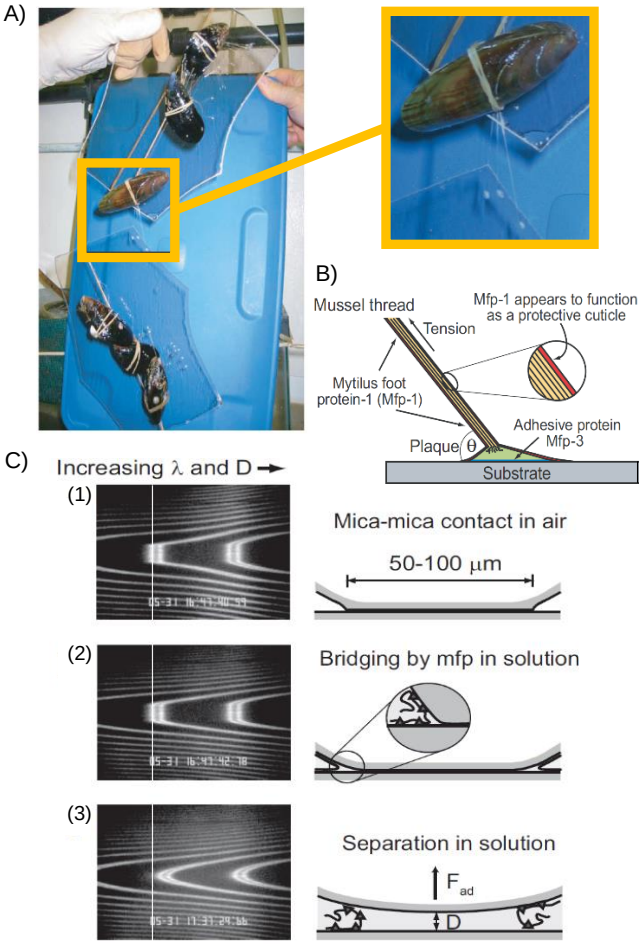

Figure 2. A) Mussels of three species adhered to mica. The enlarged image shows one of the mussels bearing the weight of a mica sheet plus three congeners by means of only three byssal threads. B) Schematic drawing of a byssal thread attached to a substrate. C) Two mica surfaces bridged by mfp-3. (*Left*) Fringes of equal chromatic order (FECO) images during an mfp-3 bridging experiment. (*Right*) Schematic drawings of corresponding molecular processes occurring at the junction: (1) Two mica surfaces in flat adhesive contact in air. (2) Same surfaces after an mfp solution was injected between them. (3) A configuration of surfaces immediately after release from adhesive contact. Reproduced with the permission from Ref. [4]. Copyright The National Academy of Sciences of the USA.

Hydrogen bonding is also relevant on metal surfaces.[41, 42] Rinderspacher et al.[43] have studied the adsorption of catechol and other phenolic compounds on hydroxylated and non-hydroxylated alumina using MD simulations. In the absence of water, a bilayer was formed on both alumina surfaces: the closest layer to the surface establishes hydrogen bonds with the aromatic rings lying flat, whereas the second layer remains upright with the hydroxyls pointing at the surface. When water was considered, catechols displaced water molecules from the substrate. In the case of non-hydroxylated alumina, the less hydrophilic surface favours hydrophobic interactions, whereas hydroxylated alumina gives rise to the strongest adsorption, mostly by cooperative hydrogen bonding with the surface

hydroxyl groups. The authors also remarked that among all the studied phenolic compounds, catechol establishes the most hydrogen bonds with the alumina surface per unit area.
Finally, hydrogen bonding has also been reported for organic substrates bearing polar groups. For instance, coating clays with polydopamine can improve their dispersibility into some polymeric matrices, though certain contributions of covalent bonding should not be completely excluded.[44,45,46] Wilker et al.[47] also studied the basic interaction of a synthetic DOPA-based polymer on different interfaces by sum frequency generation (SFG) vibrational spectroscopy. An enhanced ordering of the catechol moieties at the interface of poly(allylamine)/air was found and attributed to hydrogen bonding between DOPA hydroxyl groups and the primary amine groups of the surface polymer.

2.1.2. π-π interactions

When a catecholic species approaches an organic surface lacking polar groups, weak adsorption forces come into play. For example, Israelachvili et al.[48] have demonstrated using combined experimental and theoretical studies that van der Waals and hydrophobic interactions play an important role in the adsorption of mussel-derived peptide adhesives on wet organic surfaces. However, among the different weak interactions that can be established, π-π stacking with other π systems such as graphite,[49] carbon nanotubes (CNTs)[50,51,52,53] and graphene[54,55] deserves special consideration because of the potential technological applications of these materials.
Ruiz-Molina et al.[49] have studied the interactions of three different alkylcatechols with a highly oriented pyrolytic graphite (HOPG) surface by scanning tunneling microscopy (STM) at the solid/liquid interface. The studied molecules were synthesized bearing heptadecyl chains with the aim of favouring their ordering and stabilization on the HOPG surface. STM showed that monoalkylated species containing a bulky *tert*-butyl group, which hinders the catechol head, were unable to form structures on the surface. However, monoalkylated species lacking head hindrance formed well-defined patterns of rows with the catechol rings lying flat parallel to the surface. Thus, π interactions play an essential role in the adsorption of these alkylcatechols on HOPG since the parallel orientation of the catechol and the surface π system is needed. Finally, the strength of this interaction was also demonstrated by MD-ABF simulations, where a single molecule was transferred from the graphite to the bulk solution and the last part to leave the surface was shown to be the catechol ring.[49a]
Alternatively, Ma et al.[56] have studied the adsorption of different aromatic compounds (pyrocatechol among them) on aqueous dispersions of multi-walled CNTs and powdered activated carbon and found that π-π stacking prevailed over other non-covalent interactions, though the influence of electrostatics cannot be ruled out because of the complex adsorption trends. Similar results were obtained by Xing et al.,[57] who also studied the adsorption of several phenolic compounds on CNTs in water. The adsorption constants of the non-aromatic molecule cyclohexanol indicated significantly less affinity than those of phenol. They also concluded (supported by previous results)[58] that graphene-like surfaces act as amphoteric adsorbents, being able to interact with both π-π electron donors and acceptors. The stronger the donor/acceptor character of the molecular π system is, the stronger the π-π interaction with the surface is. Thus, catechols *per se*, having marked π electron donor character, are excellent candidates for π-π stacking anchoring elements. Taking advantage of this feature, He et al.[59] have successfully functionalized CNTs using a layer-by-layer approach with polydopamine. Characterization with transmission electron microscopy (TEM) and X-ray photoelectron spectroscopy (XPS) demonstrated that CNTs are almost fully coated with an 8 nm thin polydopamine layer that enhances their dispersibility in water and their biocompatibility. A similar approach was followed by Lee et al.[60] to achieve a good colloidal dispersion of CNTs in water, allowing for their manipulation and incorporation into conductive nanocomposite foams. In contrast, catechol-based coatings have also been used to obtain CNTs with strong hydrophobic character. For instance, Ruiz-Molina et al.[61] used the π-π stacking anchoring capacities of a polydopamine-like polymer, obtained by polymerization of an alkylcatechol with NH_3, to effectively coat CNTs. The presence of the alkyl chains provided the resulting material with hydrophobicity (Figure 3). In this case, hydrophobic interactions can be discarded as the anchoring driving force since the coating process is performed in non-polar solvents.[61] In addition, related studies with other non-catecholic aromatic systems have confirmed that π-π stacking *per se* is strong enough to achieve efficient anchoring to this kind of substrate.[52,53]

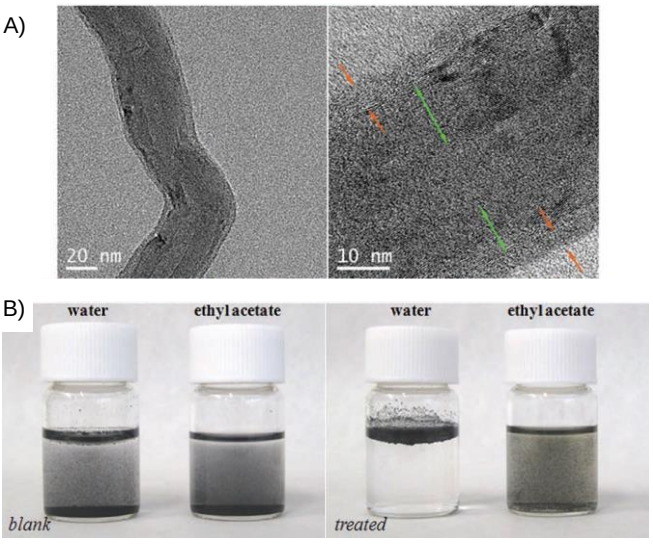

Figure 3. A) TEM images of multi-walled carbon nanotubes (MWCNTs) coated with a polymer obtained after the reaction of 4-heptadecylcatechol with NH_3. The green arrows mark the MWCNT wall; the orange arrows point at the coating thickness. B) Different behaviour of blank and treated MWCNTs dispersed in water and ethyl acetate. Reproduced with the permission from Ref. [61]. Copyright Wiley.

SFG studies of a DOPA-containing adhesive on deuterated polystyrene (d8PS)[47] demonstrated that catecholic materials can also interact by π stacking with polymeric matrices rich in aromatic rings. After the adhesive matrix was cross-linked on the d8PS surface, the intensity of SFG carbonyl peak at approximately 1663 cm^{-1} remained constant, whereas the intensity of the quinonic C=C stretching band at approximately 1610 cm^{-1} increased. The authors stated that this result indicated an enhanced ordering of the quinone rings as a result of π-π stacking with the underlying aromatic d8PS rings.
Finally, aromatic systems also strongly interact with cations.[62] Nevertheless, other than a pioneering work by Waite et al.[25] reporting cation-π interactions as a feasible adsorption driving force, catechol anchoring to surfaces by these means has not been commonly described. In contrast, this family of interactions has been consistently used to enhance the bulk cohesion of catechol-based adhesives with cations coming from both the polymer backbone itself and the medium (*vide infra*).

2.2. Chemical bonding

2.2.1. Coordination

The interaction of catechols with metallic materials occurs mainly through coordination bonds between the hydroxyl oxygens and the metal atoms of the surface with a strength that strongly depends on the metal. Though several metallic and metal oxide surfaces have been the focus of research regarding this issue, titanium oxide is one of the most widely studied because of its relevance in biomedical, catalysis, dye-sensitized solar cell (DSSC) and electrochemical applications, among others.[63]

Titanium oxide. TiO_2 is found in different forms, such as anatase and rutile. Since the underlying lattices of both structures are different, each having the possibility to present additional different face planes, specific studies should be performed for each case.[26] For example, Bowler et al.[39] developed DFT calculations to investigate the adsorption of pyrocatechol on the (100) rutile plane. The results showed that the most stable conformation is the monodentate coordination mode, whereas bidentate coordination is only favoured at defect sites where an oxygen atom has been removed from the surface. These results differ from those obtained by Diebold et al.[34] on a (110) rutile surface. The authors reported that a bidentate configuration is favoured at low surface coverages, whereas full coverages favour monodentate coordination. However, this assumption does not explain the observed experimental data, which suggested a mixed structure of alternating monodentate and bidentate coordination. Since both geometries are very close in energy, monodentate and bidentate structures could easily interconvert via proton exchange with the underlying substrate. Thus, the adsorption of catechols through coordination would not only depend on the surface but also on its coverage. Time-dependent DFT calculations[64] demonstrated that molecular adsorption by hydrogen bonding represents a less favourable situation in these systems.

Finally, combined DFT and STM studies[65] showed that isolated catechols tend to adsorb as a bridging bidentate structure parallel to the Ti_{5c} rows on the rutile surface, with the benzene ring perpendicular to the surface plane. This work also demonstrated the ability of catechols to easily exchange protons with surrounding oxygen atoms, allowing them to move across the surface. Beyond demonstrating the diffusion capacity of these molecules on rutile, these results also brought relevant information about the above-mentioned interconversion between monodentate and bidentate coordination structures.[34]
In another interesting study by Grätzel et al.,[66] the adsorption of pyrocatechol on an anatase (101) single-crystal and the crystallographically equivalent rutile (110) was compared. The authors deposited the catechol by evaporation and characterized it by XPS and near-edge X-ray absorption fine structure (NEXAFS) experiments. The authors crosschecked the collected data with DFT-optimized geometries to conclude that pyrocatechol binds more strongly to the anatase surface than to the rutile surface. Additionally, spectra obtained for O 1s suggested that pyrocatechol predominantly adsorbs at high coverages on both surfaces with a bidentate geometry (Figure 4); both pyrocatechol O atoms are chemically equivalent as they appear as only strong peak, at 531.9 eV for anatase and 531.3 eV for rutile. This hypothesis was also supported by the fact that the hydroxyl peak (532.8 eV for anatase and 532.9 eV for rutile) is small and probably includes a significant contribution from surface hydroxyl groups bonded to titanium atoms. Thus, no significant amount of monodentate coordination structures bearing unreacted hydroxyls were present.

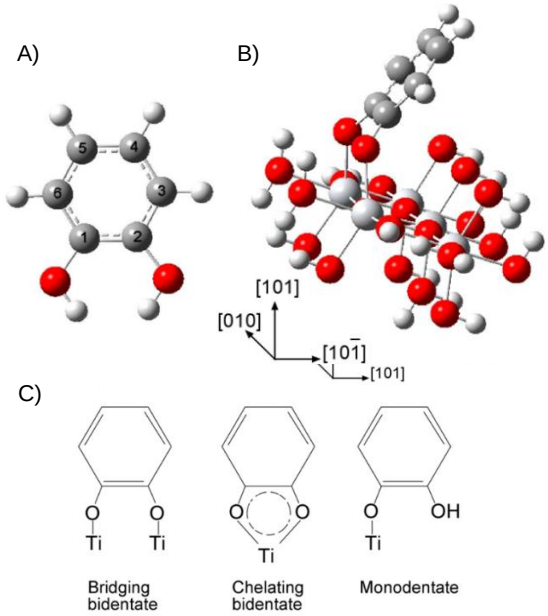

Figure 4. A) Pyrocatechol molecule (optimized geometry). Grey spheres are carbon atoms, red spheres are oxygen atoms, and white spheres are hydrogen atoms. B) A pyrocatechol molecule adsorbed on an anatase TiO_2 (101) cluster. C) Schematic picture of the three structures catechol may adopt on a TiO_2 surface. Reproduced with the permission from Ref. [66]. Copyright American Chemical Society.

Although photoemission data are not enough to differentiate bridging and chelating bidentate coordination modes, NEXAFS simulations supported the bridging bidentate adsorption as the most realistic mode. Regarding geometry, DFT calculations showed a 27 ± 6° tilting of the aromatic rings on anatase and a 23 ± 8° tilting on rutile. These data were in agreement with previous results by Diebold et al.[34], where angles of ± 15-30° to the surface normal were found using angle-resolved ultraviolet photoelectron spectroscopy (ARUPS).

Catechol derivatives with greater structural complexity than pyrocatechol have also been studied. For instance, studies of the adsorption of dopamine on anatase (101) by DFT calculations[33] and on a rutile (110) single-crystal with synchrotron XPS and NEFAXS[67] showed that the bidentate coordination is the most preferable adsorption mode on both substrates. Regarding the orientation, analysis of the NEXAFS spectra revealed that dopamine adopts an upright orientation with an angle of 78 ± 5°, twisted 11 ± 5° from the (001) direction (Figure 5). This value is higher than that previously obtained for pyrocatechol, reinforcing Grätzel's work.[68] Similar binding energies and peak distributions were found in the O 1s photoemission spectra, suggesting that dopamine also establishes bidentate coordination with titanium atoms. The main difference between pyrocatechol and dopamine was observed by combining computer modelling with NEXAFS: while dopamine molecules stand practically upright (± 5°), almost parallel to the surface normal, pyrocatechol exhibits a different tilt angle by almost 20º. This difference was attributed by the authors[67] to a higher coverage on anatase (101), which led to an increase in the steric repulsion between adsorbate molecules, thus forcing them to adopt a more vertical orientation.

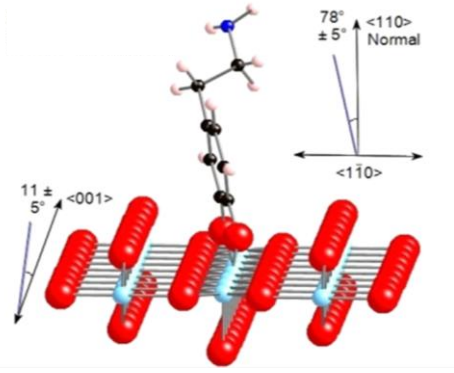

Figure 5. A dopamine molecule adsorbed on a rutile TiO_2 (110) cluster. Titanium is represented by light blue, oxygen by red atoms, carbon atoms by grey, and hydrogens by white. Reproduced with the permission from Ref. [67]. Copyright American Chemical Society.

Janković et al.[69] modified nanocrystalline TiO_2 nanoparticles with catechols bearing different donating and withdrawing groups. In all the cases, ATR-IR measurements showed that both hydroxyls of the catechol ring dissociate and bind the titanium surface in a bridging bidentate structure, as later confirmed by using Job's method. Interestingly, the dissociation constants of the complexes showed no significant differences. Therefore, though the electronic properties of the system can be tuned by the functionalization of the catechol ring, the stability of the coordination bond is not considerably affected.

Finally, with regard to the translation from discrete catechols to structures that are more complex and functional, Waite et al.[25] used QCM-D and flow ATR-IR to study the adsorption of an mfp3S-pep peptide on TiO_2 (anatase). These peptides adsorbed as a mixture of bridging bidentate coordination structures where hydrogen bonding and electrostatic interactions all contribute. In another work, Messersmith et al.[70] improved the resistance of TiO_2 surfaces to the adhesion of proteins by attaching methoxypolyethylene glycol (mPEG) strands tailored with catecholic DOPA. The authors demonstrated by XPS, spectroscopic ellipsometry (ELM) and optical waveguide lightmode spectroscopy (OWLS) that fast and irreversible coordination occurs through the DOPA moieties. Spencer et al.[71] also demonstrated the hydrophilization and hydrophobization of a TiO_2 surface by anchoring nitrodopamine and perfluoro-alkyl-nitrodopamine, respectively. Static contact angle measurements clearly showed the effect of these species on the surface, leading to contact angles of 10º and 105º for these cases, respectively. Additionally, XPS analysis clearly demonstrated that the catechol moieties coordinated the surface titanium atoms. Two different, coexisting coordination structures were found, according to the presence of two peaks in the N 1s spectra for the NO_2 group. This result was in agreement with that found for full coverages of pyrocatechol on rutile:[34] a bridging bidentate mode and a monodentate mode.

Water effects. Studies under ultrahigh vacuum conditions are essential to establish the scientific basis and understand the concepts and fundamentals behind the interactions of catechols with substrates. Nevertheless, for most real cases, the presence of water at the metal-catechol interface must be considered as it may clearly influence their interaction.[72] Therefore, different theoretical and experimental studies reporting the adsorption of catechols on different surfaces in the presence of water have been reported. All these studies showed that the adsorption energy is considerably decreased by the presence of surface water.[32,73] This phenomenon can be explained considering the energy cost associated with the removal of chemisorbed water molecules from the substrate before catechol adsorption. In addition, the presence of surface solvent molecules can also modify the structure of the final coordination complex, as demonstrated by Metiu et al.[73] *Ab initio* DFT-MD and ground-state calculations showed that pyrocatechol coordinates in the bridging bidentate mode on TiO_2 under vacuum conditions, whereas the monodentate coordination mode becomes the preferred configuration in the presence of water.

Other metallic surfaces. Though less frequent, the interaction of catechols with other surfaces has also been reported. For instance, Zhitomirsky et al.[74] studied the adsorption of caffeic acid on both rutile (110) and wurtzite, a zinc oxide commonly used for sensors and photovoltaic and optical devices. DFT calculations showed that in both cases, the most favourable coordination is a bridging bidentate structure (as previously

reported for isolated pyrocatechol molecules on TiO_2), though a higher affinity was exhibited for rutile than wurtzite. In another study, strong coordination to zinc oxide quantum dots was also observed by ligand exchange experiments. FT-IR measurements demonstrated that catechol replaces almost the 65% of the initially surface-attached acetate.[75] The authors claimed that this displacement is due to the electron delocalization caused when the two hydroxide groups originating from the dissociation of catechol hydroxyls bind to Zn(II) surface atoms.

Wesselink et al.[41] demonstrated that the mechanisms of catechol and other phenolic compounds adsorbing on different alumina forms such as gibbsite, boehmite and non-crystalline alumina were similar. FT-IR measurements showed that the catechol-surface bond is chemically affected similarly to the chelation of Al(III). From these results, the authors concluded that the dominant coordination to the alumina surfaces must be 1:1 bidentate complexation. The dominant crystal surfaces of aluminium oxides were unreactive towards catechols, and adsorption was attributed to Al-OH groups located at edge faces. Thus, non-crystalline oxides seem to be more reactive per unit area than the crystalline minerals boehmite and gibbsite. In later work,[42] the adsorption of pyrocatechol violet on boehmite in water was studied, with similar results. According to the observed stoichiometry, the catechol adsorbed on aluminium oxide coordinates as a bidentate complex rather than a monodentate complex, which is the same as the Al(III) complexes in solution.

2.2.2. Covalent bonding

Even though covalent bonding has not been as widely explored as the previously described families of interactions, there are examples of catechols covalently attaching to organic substrates. In a pioneering and conceptual study, Messersmith et al.[76] functionalized an AFM tip with a single DOPA residue. The authors studied its interaction with metal oxide and organic substrates, the latter material simulated with an amine-modified silicon surface (Figure 6). At a basic pH of 9.7, the AFM strongly attached to the surface after a certain number of pull-off cycles with a force of 2.2 nN. No adhesion was then detected in the subsequent pull-off events (Figure 6A), which could be evidence of a covalent linkage between the oxidized catechol (now in quinone form) and the amine groups of the substrate. The position of the nucleophilic attack of the amine on the quinone ring was not specified, though based on previous works, the authors stated that a Michael-type addition could occur. In a later work, SFG spectroscopy was used by Wilker et al.[47] to study the structure of a DOPA-containing adhesive at different interfaces. On poly(allylamine) (PAA), oxidized DOPA moieties established covalent bonds with the substrate. However, as the infrared signals of imines can overlap with C=C and C=O stretching and -NH_2 bending bands, these results are far from being conclusive.

In a more practical approach, Zen et al.[77] reported the covalent attachment of single pyrocatechol molecules to an organic substrate. The experiments consisted of the electrochemical modification of two types of glassy carbon electrodes under basic conditions in the presence of catecholic species. The nucleophilic groups generated on the electrodes were able to attack the *in situ*-generated quinones, most likely by a Michael-type addition. This reaction gave rise to their covalent linking, as confirmed by XPS and FT-IR measurements.

Finally, considering the small number of fundamental studies regarding the covalent anchoring of catechols to surfaces, it is worth to mention the ability of catechol-based materials to covalently attach other species. In this sense, several works can be found where polydopamine[22, 78] or polydopamine-like materials[79] are functionalized by the covalent attachment of given species. Though not directly related to the surface anchoring phenomena, such studies are examples of the covalent approach potentiality.

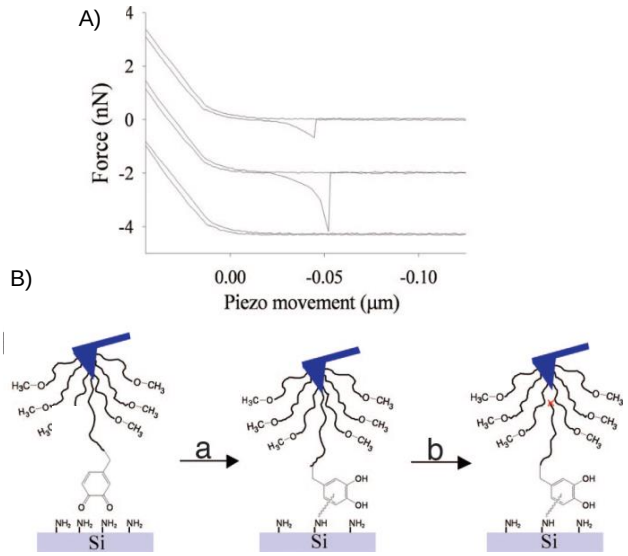

Figure 6. A) F-D curves for the interaction of a DOPA-modified AFM tip with an organic surface. The presence of DOPA was confirmed at neutral pH on Ti (top curve), showing the expected pull-off force of 800 pN. The same tip was allowed to interact with an amine-presenting organic surface at pH 9.7, which exhibited a pull-off force of 2.2 nN (middle curve). This value is consistent with covalent bond rupture. Subsequent F-D curves (after 800 contact/pull-off cycles) showed no interactions (bottom curve). B) Scheme of the covalent bond formation between DOPA and amines at the organic surface, possibly via a Michael addition-type of reaction. Reproduced with the permission from Ref. [76]. Copyright The National Academy of Sciences of the USA.

3. Beyond catechol-surface interactions

3.1. Catechol content and molecular weight

In addition to promoting surface adsorption, catechol-catechol interactions contribute to adhesive cohesion through their cross-linking. From a biological point of view, covalent cross-linking raises many doubts since the presence of quinones (obtained after oxidation of the corresponding catechol moiety) is mandatory. However, it is well known that mussels form a

reductive environment during adhesive plaque formation, precisely to prevent DOPA from oxidizing.[80] In 1999, Waite and co-workers[81] had already established the first evidence for the minority formation of quinone-derived cross-linking in mussel byssal plaques. They estimated that this reaction only occurs in 1 DOPA pair per 1800 amino acid residues (average for bulk byssal plaque material). However, covalent cross-linking is a commonly followed approach in synthetic catechol-based materials. As a general trend, larger catechol content results in greater cohesion forces. However, there is a limit; an excess of catechol may result in excessive cohesion forces, generating a rigid-like material with fewer adhesive surface interactions. In marine mussels,[7,82] optimum DOPA amounts range from 3 to 30% of total amino acid content,[83] being close to 10 mol% on average.[84,85] Based on this observation, several groups focused on the synthesis of catechol-based adhesive materials with optimized catechol contents.[86,87,88,89,90,91] Mussel-inspired biomimetic polymers have been mainly prepared from polyesters,[88,89] polyamides,[92] polyacrylates,[93,94,95,96] polyethylene glycols,[16,97,98,99] polyoxetanes,[87,91] polystyrenes[86,100] polypeptides[101,102,103] and polysaccharides.[104,105] The results defined a range of optimal catechol content close to that observed in mfps but with differences depending on the nature of the material used. However, despite this growing number of synthetic polymers mimicking mussel adhesive proteins, the number of detailed and systematic studies aimed at elucidating this issue is rather limited. This lack of studies and the wide variety of catechol-based polymers, techniques used for measuring adhesion, substrates, environments of operation and curing conditions, make any conclusive and realistic comparison under standard conditions difficult. For instance, the use of oxidative cross-linkers generally enhances bulk adhesion.[86-89,91,100,106] However, Stuart and Kamperman[90] described the opposite effect for dopamine methacrylamide (DMA) and 2-methoxyethyl methacrylate (MEA) (Figure 7).

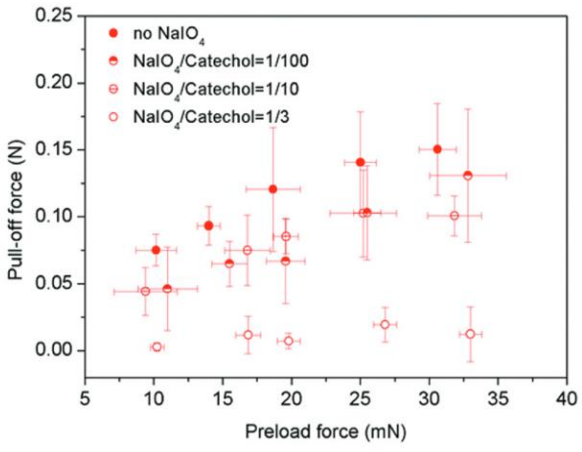

Figure 7. Dry adhesion of P(DMA0.05-*co*-MEA0.95) in the presence of an oxidant ($NaIO_4$). Each data point resulted from an average of three to five measurements. Reproduced with the permission from Ref. [90]. Copyright Royal Society of Chemistry.

Thanks to their chemical structures, the chains of these polymers with enough cohesion forces interact to a high degree. However, the gradual addition of small amounts of $NaIO_4$ progressively decreased the adhesion of the materials until their total disappearance. The authors claimed that I) some of the catechols were oxidized to quinones, which significantly lowered the adhesion,[38] and II) the addition of cross-linkers to the polymer considerably increased the stiffness.[96]

To the best of our knowledge, the lowest optimum catechol content within a polymer to induce strong adhesion ranges from 5-8 mol% for a polylactic acid-based polymer,[75,88,89] dopamine methacrylamide-based polymer[90] and bis-phosphate ester grafted oxetane-based polymer.[91] These polymers can establish hydrogen bonds or van der Waals forces within the material, increasing cohesion and cross-linking. Hence, less catechol is required to obtain higher overall adhesion. In contrast, one of the highest catechol contents (approximately 30-33 mol%,) was used for polystyrene-based polymers,[86,100] where weaker interactions between polystyrene macromolecules occur. In between these extremes, several works report optimum catechol contents close to 10-15 mol%.[85,87,107]

This parameter is also strongly dependent on the polymer molecular weight (Figure 8).[100]

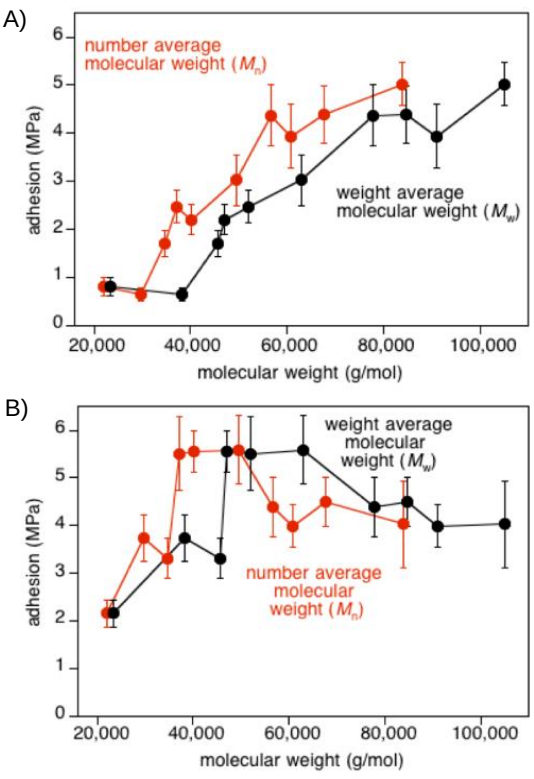

Figure 8. Effect of molecular weight on the adhesion of poly[(3,4-dihydroxystyrene)-co-styrene] before (A) and after (B) cross-linking with $[N(C_4H_9)_4](IO_4)$. The number average molecular weight (Mn) is shown in red, and the weight average molecular weight (Mw) is depicted in black. Adhesion testing was conducted in shear on aluminium substrates. Reproduced with the permission from Ref. [100]. Copyright American Chemical Society.

Overall, low molecular weight species have better mobility and therefore provide better wetting for enhanced surface interaction.[108] However, this improvement is countered by decreased cohesiveness. In contrast, higher molecular weights effect supplementary chain entanglements that contribute to increased cohesive bonding.[109] This concept was nicely shown by Wilker et al.,[100] who studied the effect of molecular weight in poly[(3,4-dihydroxystyrene)-co-styrene] while maintaining a 30 mol% catechol content with and without the addition of cross-linkers.[86] The authors concluded that the absence of cross-linkers generally results in higher adhesion for polymers with higher molecular weights. However, the addition of $(Bu_4N)IO_4$ as a cross-linking agent has the opposite effect; under these conditions, greater adhesion is exhibited by polymers with lower molecular weights. On the other hand, if a copolymer based on polystyrene was replaced by polylactic acid, much less catechol was required to achieve high bulk adhesion (approximately 7 mol%), despite having a lower molecular weight.[87] As the authors noted, a smaller amount of catechol moieties is needed thanks to the stronger interchain interactions between polylactic acid strands than between polystyrene chains.

3.2. Roles of other functional groups in the polymeric backbone

Beyond catechol, the presence of other species such as cationic, anionic, non-ionic polar and non-polar functional groups are also relevant in the wet adhesion of mfps.[110] Accordingly, novel approaches to incorporate some of these functionalities in order to achieve synergism with catechol derivatives have been developed mainly in two specific areas: I) surface or structure conditioners and II) cross-linkers, most of which are analysed next in more detail.

Surface and structure conditioners. The success of synthetic adhesives in wet environments is most often conditioned by a previous cleaning of the substrates, either by chemical treatments and/or partial drying.[101] An interesting alternative to avoid this preliminary step is the introduction of surface conditioners within the polymeric backbone to improve the close contact with the surface. The objective is to minimize the effect of detrimental agents such as certain solvents or salts. For instance, several works have demonstrated that the presence of cationic groups (such as iminium, ammonium or guanidinium groups) in the material backbone significantly enhances its underwater adhesion (Figure 9), [101,111,112,113,114,115,116,117] which is primarily the result of surface salt displacement from the substrate because of the competition with the cationic groups included in the polymer backbone. The flexibility and length of the cationic and the catecholic groups as well as the distance between them are crucial for the adhesion enhancement.[113,115] Finding the optimum charge is challenging as an excess can be detrimental due to I) the prevalence of charge-charge repulsions or II) competition between cationic and catechol moieties for negative surfaces.[111,117,118]

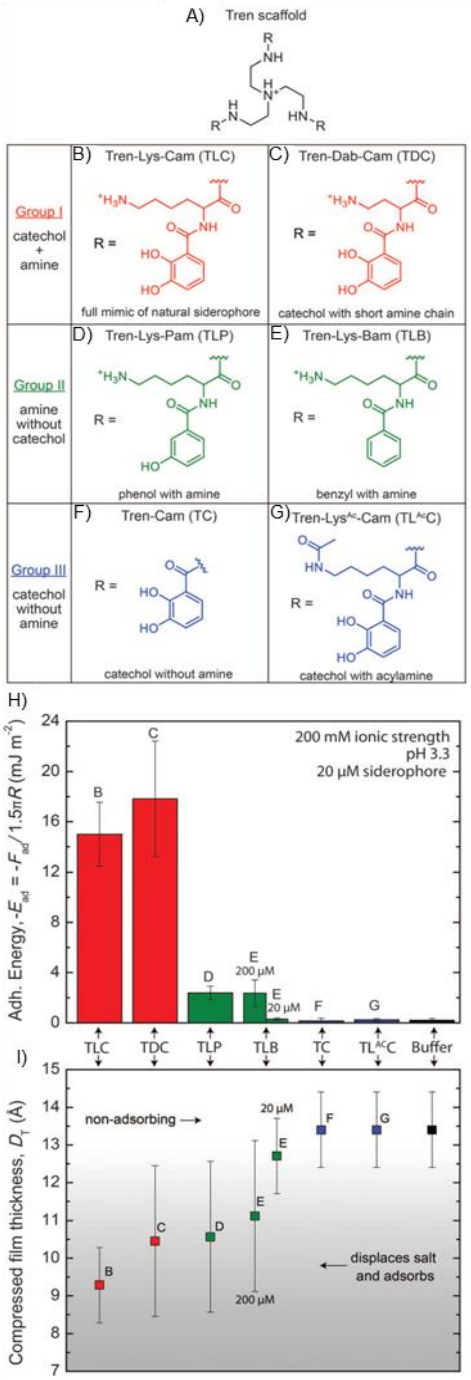

Figure 9. The synergy of catechol and lysine (Lys) in siderophore adhesion. A) Structure of the Tren scaffold. B to G) The R groups appended to Tren. H) The average adhesion energy required to separate two mica surfaces adsorbed with 1 nmol (20 mM, except where indicated at 200 mM) of the homologue in buffer at pH 3.3 after 10 minutes of contact. I) D_T of the siderophore monolayer between two mica surfaces at 10 mN/m compressive load. The film thicknesses correspond to the adhesion energy displayed in (H). A decreased film thickness (<12 Å) indicates that homologues B, C, D, and E (200 mM) adsorb, displace hydrated salt at the mica surface, and mediate adhesion between two mica surfaces. Reproduced with the permission from Ref. [113]. Copyright Science.

Balances of hydrophilic/hydrophobic forces are also relevant for favouring interactions with surfaces. For example, if the polymer backbone is hydrophobic (such as that of polystyrene or polyoxetane), it tends to avoid hydrophilic surfaces, weakening the binding of the catechol moieties.[119] In this way, the design of copolymers containing catechol residues located between hydrophilic blocks (e.g., PEG and polyvinylpyrrolidone (PVP)) ensures good wetting or adhesive contact (biologic scaffolds and tissue/implant surfaces).[120,118,119] Conversely, the inclusion of DOPA in a hydrophobic aromatic sequence prevents catechol moieties from being exposed to the surrounding aqueous environment, retarding their oxidation.[121]

Cross-linkers. Strong or weak nucleophiles in the polymeric chain, such as amines or thiols, can react with oxidized catechols through Michael-type additions or Schiff base reactions (Figure 10).[122,123] This process enhances the cohesion by means of covalent cross-linking. Furthermore, some functional groups such as protonated amines can also establish cation-π interactions, which represent one of the strongest non-covalent interactions in water.[62] Cation-π interactions enhance the adsorption of catechols to charged surfaces[124] and the cohesive properties of materials rich in aromatic and cationic functional groups.[125] These interactions can also complement the weaker adhesion of the quinone moieties in oxidizing environments. This supplementation enables interfacial contributions that assist material-independent adhesion,[126] particularly between protonated nitrogen-based groups (cation donors) and polyindolic rings (π donor).[114,127]

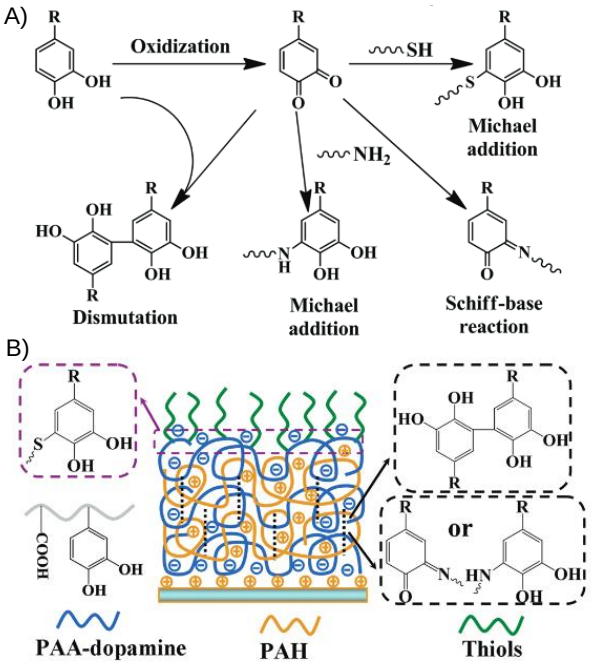

Figure 10. A) Catechol oxidative chemistry explored from mfp and B) a stable functional multilayer film prepared by the integration of catechol oxidative chemistry into layer-by-layer assembly. PAH is poly(allylamine hydrochloride), and PAA is poly(acrylic acid). Reproduced with the permission from Ref. [123]. Copyright American Chemical Society.

Finally, thiol groups also improve adhesive strength by the oxidation of sulfhydryl groups to disulfide bonds or, more specifically, through a click thiol-ene reaction.[128,129] Independently of the type of interaction, a significant increase in the cross-linking necessarily encompasses significant catechol consumption and therefore a reduction of surface adhesion. This problem has been circumvented on mussels limiting DOPA oxidation during adhesive plaque formation by imposing an acidic medium based on the thiol-rich protein mfp-6, which restores DOPA by coupling the oxidation of thiols to dopaquinone reduction.[128] Mimicking this strategy, some authors have established alternative approaches based on the use of synthetic adherers with a low pK_a to favour cross-linking at an acidic pH and/or reduce the quinone back to catechol to improve adhesion.[80] For example, thiourea derivatives, which are excellent nucleophiles and exhibit convenient reducing power under acidic conditions, have been used to improve the adhesion properties of catechol-conjugated gelatin hydrogels. Also in this context, electron-withdrawing groups (such as chlorine and nitro), which decrease the pK_a of the catecholic hydroxyls, can lead to higher reactivity towards nucleophiles found on tissue substrates, even at mildly acidic pH values. This change results in a significant increase in the interfacial binding strength of catechols under acidic conditions since they are minimally hampered by pH changes.[1,130]

3.3. pH and redox: the balance between adsorption and cohesion forces

The redox transition of catechols to quinones upon a pH increase and/or the addition of an oxidant is fully established.[131] In the previous sections, the mechanism by which the catechol moiety is mainly responsible for the adhesiveness of catechol-based materials via either non-covalent interactions (Section 2.1) or chemical bonding (Section 2.2) has been shown. However, cohesion comes from the ability of the reactive quinone state to generate cross-linked structures, mainly in synthetic materials (Section 3.1). Within this context, acidic and neutral pH values are necessary to ensure the proper fraction of the catecholic form (Figure 11).[132,133,76] In contrast, basic pH values enable cross-linking, which is necessary to achieve well-adjusted cohesiveness. Achieving a proper pH balance is therefore crucial to ensuring optimized adhesion/cohesion ratios and has become the focus of research groups.

Waite and co-workers[134] have used an SFA to determine the force-distance profiles and adhesion energies of mfp-3 on a TiO_2 surface at three different pH values (pH 3.0, 5.5 and 7.5). The results showed that the strongest adhesion occurs at pH 3. An increase of the pH to 5.5 decreases the measured adhesion forces. However, a further increase to 7.5 recovers the original adhesion value. This behaviour was rationalized as a balance between two opposing simultaneous effects during the pH variations: I) DOPA oxidation, which diminishes the adhesion, and II) the binding of a single DOPA molecule to the TiO_2 surface, which changes from hydrogen bonding to coordinative bonding, thus increasing the binding strength. The same authors also investigated the pH dependence of the adhesion of the

electrophoretically slow protein mfp-3 (a hydrophobic variant with a smaller percentage of DOPA than the fast variant). At pH 3, where DOPA is stable, both proteins showed similar behaviour, with adhesion to mica proportional to the molar percentage of DOPA. At pH 5.5 and 7.5, however, the adhesion of the mfp-3 slow was almost half of that found for the mfp-3 fast, suggesting that DOPA in mfp-3 slow is less prone to oxidation. Accordingly, cyclic voltammetry measurements proved that the oxidation potential of DOPA in mfp-3 slow is significantly higher than that in mfp-3 fast at pH 7.5. This effect is attributed to the high proportion of hydrophobic amino acid residues near DOPA.[121] In a related study,[110] synthetic copolyampholytes have been obtained and formulated as coacervates for adhesive deposition on surfaces. The synthetized copolyacrylates combine catechol units with amphiphilic and ionic functionalities present in mfp-3 slow. Some of these copolymers formed coacervates at pH 4 and showed strong adhesion to mica. Increasing the pH to 7 after coacervate deposition doubled the bonding strength without oxidative cross-linking. UV-visible spectra of the materials showed similar signals at different pH values; quinone absorption bands were not observed. The authors claimed that this is an example of how hydrophobic residues in the copolymer can provide stability against catechol oxidation.

Reches et al.[133] also performed a systematic study of the pH effect on the rupture forces between DOPA and related amino acids and a chemically well-defined TiO_2 surface using single-molecule force spectroscopy (SMFS). At neutral pH values, DOPA presented a single strong average adhesion value of 383 ± 21 pN, in concordance with previous reports on the strong binding of this species to inorganic surfaces.[76] In basic medium (pH 9.8), DOPA showed a bimodal force distribution with average adhesion force values of 108 ± 31 pN (75%) and 362 ± 21 pN (25%), which were attributed to dopaquinone and DOPA, respectively. The study also evaluated the influence of DOPA substituents in the adhesion. At neutral pH values, interaction forces for *N*-Boc-6-hydroxy-L-DOPA were slightly higher than those of DOPA. However, in the case of *N*-Boc-6-nitro-L-DOPA, a bimodal force distribution was obtained with similar values and distributions to those obtained for DOPA at basic pH (Figure 11). In a work by Lee and co-workers,[135] the effect of pH on the intermolecular cross-linking rate of a 4-armed dopamine-terminated PEG was studied. Such hydrogels formulated at slightly acidic pH values (between 5.7 and 6.7) experienced a reduced curing rate after periodate oxidant addition, exhibiting poor mechanical and adhesive properties. At pH 8, an increase in the curing rate was observed. However, the resulting materials again showed a limited mechanical and bioadhesive performance. Finally, adhesive hydrogels formulated at pH 7.4 were obtained at a faster curing rate with a good balance between efficient interfacial binding and mechanical properties. The evolution of the chemical species resulting from addition of the oxidant agent was tracked using UV-visible spectroscopy. This technique revealed that the stability of the quinone intermediate generated by the oxidation of dopamine increases under acidic conditions.

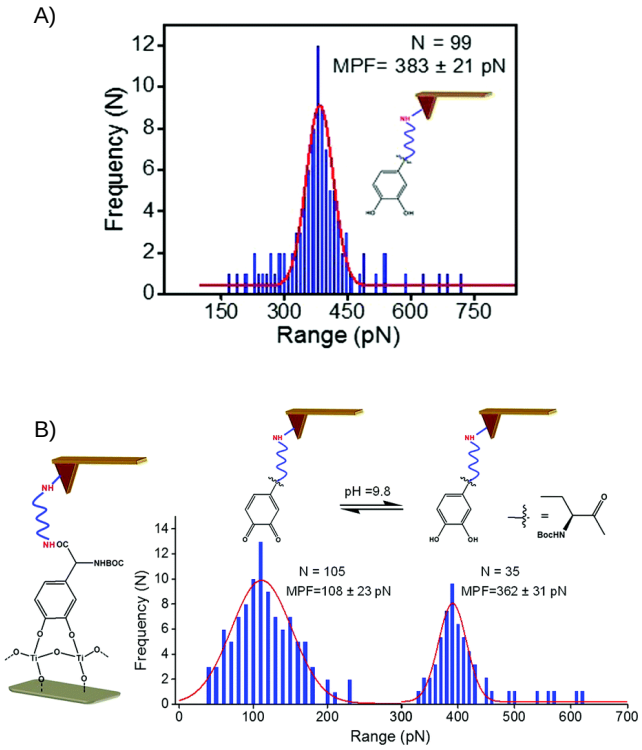

Figure 11. A) Histogram of the rupture force values between DOPA and the TiO_2 surface (loading rate of 4.6 ± 0.7 nN/s in Tris buffer (50 mM, pH 7.2)). B) Histograms of the forces required to rupture DOPA from the TiO_2 surface at a loading rate of 4.5 ± 0.6 nN/s in Tris buffer (50 mM, pH 9.8). The strong interactions are assigned to the non-oxidized DOPA (DOPA-enol) and TiO_2, whereas the weak interactions are assigned to dopaquinone and TiO_2. Reproduced with the permission from Ref. [133]. Copyright Royal Society of Chemistry.

Researchers have also developed different strategies to cross-link polymers at acidic pH values by introducing additional moieties[80a] or diminishing the pK_a value of the catecholic hydroxyls.[130] Other works have published an intelligent approach based on boronate-catechol complex formation and its pH-dependent reversibility. Waite and co-workers[136] followed this strategy with a twofold objective: I) retard DOPA oxidation at neutral pH and II) maintain adhesive properties under oxidizing conditions through the dissociation of the complex. In another work, Lee and co-workers[137] described the preparation of pH-responsive adhesive hydrogels by copolymerization of dopamine methacrylamide and 3-(acrylamido)phenylboronic acid. These materials showed great adhesive properties at pH 3 that were drastically reduced at pH 9. At acidic pH values, the catechol and borate moieties contributed to strong interfacial binding with the substrate; at basic pH values, the formation of an internal boronate-catechol complex occurred (as confirmed by means of FT-IR and rheometry measurements), reducing the adhesive properties of the hydrogel. This process was demonstrated to be reversible for several pH changes.

In a more recent work, Sohn and co-workers[138] studied pH-responsive silica nanoparticles functionalized with catechol-modified hyaluronic acid (HA-CA) (Figure 12). The competition between adhesive and cohesive forces within the material led to the formation of three different structures: I) an unstable catechol-modified HA-CA shell at pH 5.5; II) monodisperse spherical silica HA-CA-coated particles at pH 7.4; and III) an amorphous HA-CA layer at pH 8.5. This behaviour was a consequence of the pH-dependent redox transition of catechol, affording strong adhesion of HA-CA to silica at pH 5.5 and structural cohesiveness at pH 7.4. The chemical composition of HA-CA was analysed by FT-IR. As expected, the C=O stretching vibration at 1715 cm^{-1}, attributed to the quinone state, was mainly measured at pH 7.4. The influence of pH on the catechol to quinone transition was also measured using XPS and showed the variation of representative C-C/C-H and C=O species when the pH was increased.

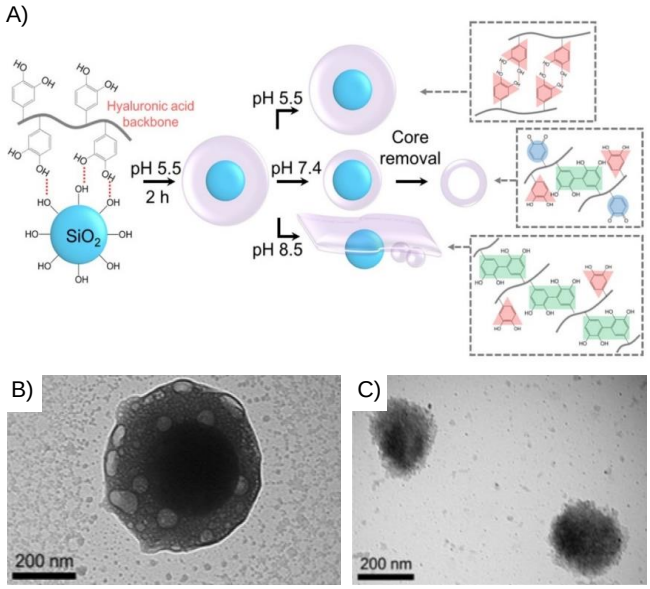

Figure 12. A) Schematic illustration of silica@HA-CA formation at different pH values: I) an unstable catechol-modified HA-CA shell at pH 5.5, II) monodisperse spherical silica HA-CA-coated particles at pH 7.4, and III) an amorphous HA-CA layer at pH 8.5. B) Bio-TEM image of silica@HA-CA particles at pH 7.4 and C) Bio-TEM image of hollow silica@HA-CA particles at pH 7.4 after silica core removal. Reproduced with the permission from Ref. [138]. Copyright Elsevier Ltd.

Finally, Wilker et al.[139] focused on the rich redox chemistry taking place in mussel wet adhesion to rationally design and develop new antifouling coatings for ships. The addition of the usual antioxidants that are insoluble in water to a commercial ship coating decreased mussel adhesion to aluminium plaques in artificial seawater (pH 7.9). Interestingly, a correlation was established between decreased adhesion and a low electrochemical potential of the antioxidant. This result may indicate that these species disrupt the curing of mfps by reducing quinone intermediates to the catechol state.

3.4. Presence of ions

The mfp adhesion process occurs in two stages:[140] I) catechol anchors to the surface and II) a slow (1-4 hours) curing process where extensive cross-linking within the protein occurs. The objective for the cross-linking is twofold: improving the mechanical performance of the threads and the formation of adhesive plaques.[141] In addition to the covalent interactions described in the previous sections, cross-linking through transition-metal ions represents the most used mechanism.[142] In fact, mussels concentrate metal ions such as iron, zinc, copper, and manganese from seawater [143] into their adhesive at levels much higher than those found in open ocean waters.[144] For this concentration to happen, metal ions coordinate to the dianionic catecholates of mfps to form mono-, bis-, or tris-coordination complexes, depending on the valency of the metal ion, catechol-to-metal ion molar ratios and pH.[145] In contrast to covalent cross-linking, metal-ligand coordination is reversible, thus giving elasticity and self-healing properties to the mfps.[146] Besides cross-linking, metal ions also facilitate the adhesion of catechols to different surfaces. The roles of the previously studied metal ions are described next.

Iron. The cross-linking of mfps in the presence of Fe(III)[147] is quite strong. The DOPA-Fe(III) complex exhibits very high binding and stability constants, and the bond can be reversibly broken.[148] A Raman microscopy map of DOPA coordination to Fe(III) throughout the byssal plaque has evidenced a predominance of iron in the outer cuticle and central bulk of the plaque, where mfp-1 and mfp-2 are the prevalent proteins. In contrast, less iron was found near the interface between the plaque and the substrate, where mfp-3 and mfp-5 are predominant. There is a reason for this distribution: for mfp-1 and mfp-2, which form the cuticle and the central bulk of the plaque, respectively, the prevalence of Fe(III)-DOPA complexation is essential for their structural integrity and unique mechanical properties[149, 150] as this complexation provides hardness, extensibility and self-healing properties.[151] No involvement in a specific physiological function is known.[152] Additionally, fluorescence microscopy and elemental analysis have demonstrated that Fe(III) and Ca(II) coexist in mfp-1 in the cuticle of *Mytilus galloprovincialis* byssal threads, leading to the proposal of Ca(II) having similar functions to Fe(III). In fact, chelation and the removal of both ions from the cuticle resulted in 50% hardness reduction and a disruption of cuticle integrity.[153] In contrast, whereas the role of the DOPA-Fe(III) bond in mfp-1 and mfp-2 is well-established, its function in mfp-3 and mfp-5 remains unclear, especially considering their role at the byssus/surface interface.[154]

In addition to being a coordinative cross-linker, Fe(III) also induces DOPA oxidation and subsequent aryl cross-linking during mfp curing.[155] Electron paramagnetic resonance (EPR) of mfp-1 and mfp-2 precipitated upon addition of Fe(III) at acidic pH values revealed the presence of radical species. These species were assigned as both a high-spin Fe(III) and an organic radical, presumably DOPA-semiquinone, which is known to undergo aryl coupling.[131] These results are also supported by

theoretical calculations that demonstrated that the strength with which Fe(III) coordinates the catechol ligand is not particularly strong. Therefore, the strong cross-linking in the presence of Fe(III) can be ascribed to this ion's additional ability as an oxidant to induce covalent coupling of the catecholic groups of mfps.[156]

In addition to the fundamental studies previously described, several other revisions have highlighted the role of iron in the adhesive properties of mfp-inspired materials.[140] Such works include AFM studies,[157] binding of DOPA-containing mfps[158] and hydrolysed peptides,[159] spectroscopic and chemical characterization of the complexes formed during cross-linking[160] and metal-mediated cross-linking in mfps.[161] In a recent study, Cha et al.[162] confirmed DOPA-Fe(III) complexation in mfp-3F and mfp-5 and investigated its effect on both cohesion and surface adhesion (Figure 13). At low pH values (similar to those of the local acidic environments during the secretion of adhesive proteins), DOPA-Fe(III) complexation decreases. Under these conditions, SFA measurements showed strong surface adhesion and weak cohesion. Alternatively, higher pH values (similar to those found in seawater) favour catechol deprotonation and thus the formation of more iron-catechol bonds and a consequent remarkable increase in cohesion forces.

All the fundamental knowledge regarding the role of iron in the adhesion properties of byssal threads[163] has fuelled the development of novel materials and applications, e.g., surgical adhesives and orthopaedic cements,[164] versatile metal-phenolic platforms used to engineer nanomaterials and biointerfaces,[165] dendritic polymers as universal multifunctional coatings[166] and novel hydrogel actuators inspired by the reversible mfp chemistry.[167]

The reversibility of the DOPA-iron bond has also been used to fabricate self-healing hydrogels with stretching capacities ten times their original lengths.[168] This high extensibility can be completely recuperated in under 20 min, even after they've been cut apart. In addition, the hydrogels respond to multiple stimuli such as mechanical force, temperature, and certain chemicals because of the dynamic catechol-Fe(III) bond. In another example, polyoxetane copolymers with grafted catechol moieties showed strong bonding upon addition of $FeCl_3$ as a cross-linker. Polymers containing up to 15.5 mol% catechol content showed the strongest bonding to a variety of substrates, including sanded stainless and porcine skin.[87]

Chelation with iron can even favour much higher bonding strength in seawater than under dry conditions. Wan et al.[119] reported a catechol-containing PVP backbone that upon addition of $FeCl_3$, increases in bond strength to a maximum of 1.63 MPa (average: 1.33 MPa). The authors argue that there are two main reasons for this outstanding adhesion: I) amides within PVP establish additional hydrogen bonds with the substrate, working together with catechols to repel water molecules from the surface, and II) water and Fe(III) slowly diffuse into the polymer thanks to the hydrophilic character of the PVP backbone, thus promoting a more homogeneous coordination cross-linking.

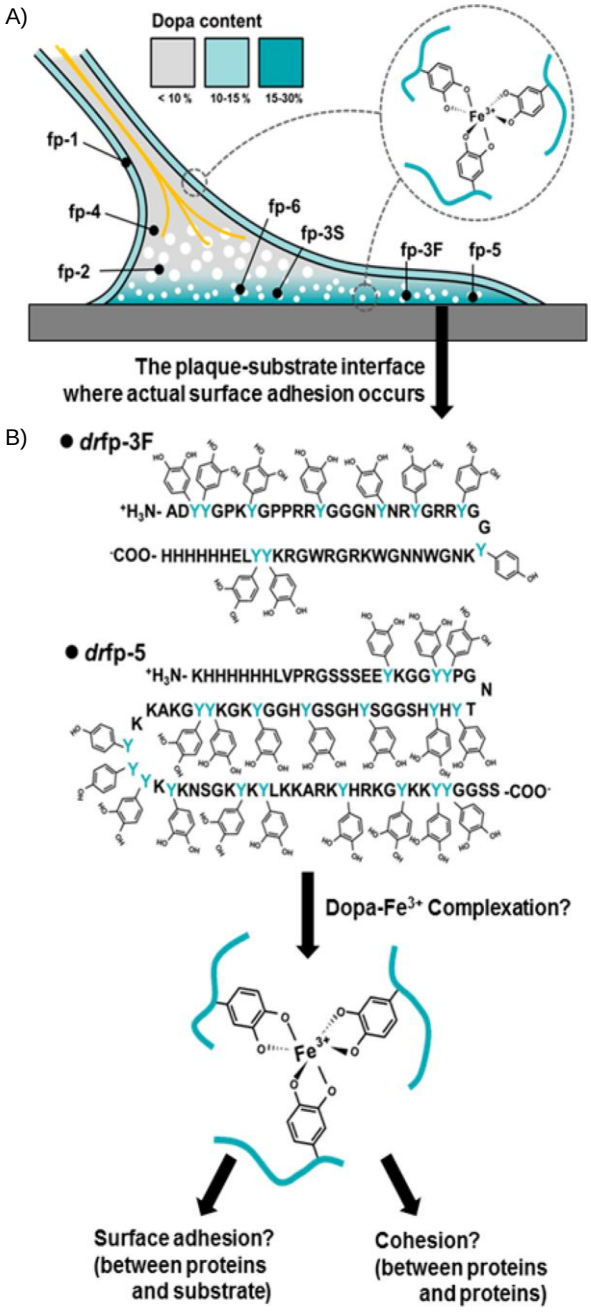

Figure 13. A) Schematic illustration of mussel byssus showing the location of mfp-1-6 proteins and the relative content of DOPA, as indicated by the colour gradient. Mfp-3F and mfp-5 are located at the plaque substrate interface mediating surface adhesion. DOPA-Fe(III) complexes are found everywhere on the byssus from interface to cuticle. B) Amino acid sequence information for DOPA-incorporated recombinant foot proteins 3F and 5 (drfp-3F and drfp-5); ~94% DOPA incorporation yield indicates that almost all tyrosine residues were converted to DOPA. Reproduced with the permission from Ref. [162]. Copyright American Chemical Society.

Finally, proper amounts of dopamine and metal ions endow an epoxy adhesive with better water resistance and excellent adhesion properties.[106] The authors found that though dopamine itself increases the adhesion strength of a material and its resistance to water, complexation with Fe(III) (for a dopamine content less than 5 wt%) further improves its performance. UV-visible and X-ray diffraction measurements confirmed that at high dopamine-Fe(III) ratios, bis-catecholate complexes are formed, favouring cohesion and thus the overall adhesion.

Copper and manganese. QCM-D, dynamic light scattering (DLS) and small-angle X-ray scattering (SAXS) have been successfully used to study the intra- and intermolecular cross-linking of mfps with different metal ions.[169] Specifically, the viscoelastic properties of the *M. edulis* foot protein Mefp-1 adsorbed on modified hydrophobic gold surfaces after the addition of Cu(II), Mn(II) and $NaIO_4$ were studied. The reduction in viscoelasticity followed the order $NaIO_4$ > Cu(II) > buffer control > Mn(II). While Cu(II) participates in intermolecular cross-linking via metal complexation and increases the abrasion resistance of the Mefp-1 layer, $NaIO_4$ mainly resulted in the intramolecular formation of di-DOPA cross-links, thus failing to induce larger intermolecular aggregation. In a related work, the comparative adsorption of the Mefp-1 cross-linked with $NaIO_4$ and catechol oxidase on two different surfaces was studied via surface plasmon resonance (SPR) and QCM-D. A negatively charged polar SiO_2 surface and an electrically inert non-polar CH_3-terminated thiolated gold surface were used. Upon cross-linking of the Mefp-1 formed on the CH_3 surface, the rigidity of the adlayer(s) increased significantly. A similar increase in the rigidity was also observed upon addition of Cu(II), suggesting that the high level of metal ions present in the byssus thread might be essential for the cohesive and adhesive contributions of this protein.[170]

Others. Harrington and co-workers[171] have demonstrated that different metal ions are equally sufficient as DOPA cross-linking agents. The authors performed the *in vitro* removal of native DOPA-metal complexes using ethylenediaminetetraacetic acid. After replacement of the metals with vanadium or aluminium, the cuticle performance does not suffer significant changes, preserving most of the stiffness and hardness of the material (above 80% in both cases). Wilker et al.[172] also studied the role of other metals in the cured glue of marine mussels. For this work, proteins containing DOPA were extracted from mussel feet and mixed with potential cross-linkers, including metal ions (e.g., Na(I), Zn(II)), oxidizing transition metals (e.g., Fe(III) and $Cr_2O_7^{2-}$), non-metallic oxidants (e.g., H_2O_2, IO_4^-), and oxidizing enzymes (e.g., tyrosinase)). The compressibility and shear properties of the resulting materials were investigated by means of a penetration test, and the results showed optimal curing with oxidizing metal ions.
Finally, Ni(II) amends the polymerization kinetics of polydopamine.[173] Spectroscopic and electron microscopy studies revealed that chelation occurs, forming homogeneous Ni(II)-dopamine complexes and thus accelerating the assembly of dopamine oligomers in polymerization.

4. Summary

Several studies in the literature aimed to understand the adhesion properties of catechol-based materials. On grouping all these examples, one should consider two main different factors, both crucial for optimal performance and requiring adequate balancing: I) adsorption of the catechol moiety on the surface (valuable for both coatings and adhesives) and II) cohesion of the whole material by cross-linking (mainly for adhesives).

Adsorption. Catechol establishes numerous interactions (both non-covalent forces and chemical bonding) whose prevalence depends on the nature of the substrate to be attached. For instance, thanks to the presence of the two neighbouring hydroxyl groups, catechols can anchor to inorganic surfaces by means of hydrogen bonding (mainly inorganic substrates lacking transition metals, such as silica and mica) or coordination (on metal oxides, preferentially at defect sites where undercoordinated metal atoms favour the dissociation of hydroxyl groups and coordination to the metallic centre). These interactions, even non-covalent ones, are strong enough to displace preadsorbed water molecules, allowing the catechols to adsorb in wet environments. In addition, the torsion capacity of these hydroxyls seems to be responsible for an enhanced capacity to adapt to the underlying surface lattice, which would improve the efficacy of the interaction. On the other hand, the catechol benzene ring allows for establishing different interactions with organic surfaces, such as π-π stacking, which is of relevance mostly when catechols approach substrates rich in aromatic systems (e.g., graphene, CNTs or polymers containing aromatic groups). In these cases, though hydrophobic interactions can also mix and contribute to these supramolecular entities, π interactions alone are effective, even in non-polar solvents. Beyond π-π stacking, covalent bonding is also an interaction between catechol and organic substrates. In these cases, catechols must be oxidized to the quinone form to favour the nucleophilic attack of groups such as amines or thiols. A relative ease in undergoing redox processes would be a key factor in favouring this anchoring strategy.
Finally, it is important to remark that in most cases, the coexistence of different adsorption modes occurs. Thus, exclusivity should not be generally expected in catechol-surface interactions.

Cohesion. Cohesion can be modulated by different factors such as catechol content and the presence of specific functional groups in the material backbone. While the influence of the catechol content has been clearly identified, no specific correlation between this content and adhesion has been established due to the many relevant influential variables. Alternatively, the presence of strong or mild nucleophiles such as amines or thiols in the polymeric chain can enhance the degree of cross-linking and hence cohesiveness.
Factors external to the adhesive material itself, such as pH or the presence of metal ions, also modify the adsorption/cohesion properties of the material. For instance, pH determines the redox balance between the catecholic and quinonic forms and thus the

compromise between adsorption and cohesion capacities. As a general trend, a large amount of the catecholic form favours adsorption at the expense of cohesion and vice versa. Nevertheless, this trend should not be extrapolated to organic substrates, where interfacial quinones in the adhesive material play a crucial role as anchoring agents through covalent bonding. On the other hand, cohesive cross-linking relies on not only the quinonic state but other factors since different metal ions can interact with catechol moieties, enhancing the cohesiveness by coordination. This strategy is observed in Nature, where mussels concentrate ionic species such as iron, zinc, copper, and manganese from seawater into their adhesive proteins at levels much higher than those found in oceans. Besides playing an active role as coordination cross-linkers, metal ions also lead to the formation of semiquinones. These semiquinones react through a radical-radical mechanism, giving rise to covalently cross-linked species. However, an excessive degree of cross-linking (either covalent or coordinative) can be detrimental because it may lead to an extremely stiff material and consequent adhesion decrease.

In summary, the roles of catechols and other agents (both inherent and external to the material) have been determined in the optimal balancing of the adsorption/cohesion equilibrium and thus in overall adhesion. This review established a comprehensive toolkit of such factors from a chemical point of view and definitely provides readers a better understanding of these materials, which should therefore lead to an improvement of their properties. In other words, this review is aimed at being a road map towards novel catechol-based adhesives. However, the application of the information in this review is not straightforward and should be considered on a case-by-case basis mainly depending on the nature of the substrate and the conditions of the surrounding environment.

Acknowledgements

This work was supported by project MAT2015-70615-R from the Spanish Government and by FEDER funds. The ICN2 is funded by the CERCA programme/Generalitat de Catalunya. The ICN2 is supported by the Severo Ochoa programme of the Spanish Ministry of Economy, Industry and Competitiveness (MINECO, grant no. SEV-2013-0295). We would like to thank J. Sedo for fruitful discussions.

Keywords: catechol • mussel • adhesion • polydopamine

[1] C. J. Sun, A. Srivastava, J. R. Reifert, J. H. Waite, *J. Adhes.* **2009**, *85*, 126.
[2] J. -L. Jonker, L. Morrison, E. P. Lynch, I. Grunwald, J. von Byern, A. M. Power, *Interface Focus* **2005**, *5*, 20140062.
[3] K. Kamino, *Biochem. J.* **2001**, *356*, 503.
[4] Q. Lin, D. Gourdon, C. Sun, N. Holten-Andersen, T. H. Anderson, J. H. Waite, J. N. Israelachvili, *Proc. Natl. Acad. Sci. USA* **2007**, *104*, 3782.
[5] L. Petrone, A. Kumar, C. N. Sutanto, N. J. Patil, S. Kannan, A. Palaniappan, S. Amini, B. Zappone, C. Verma, A. Miserez, *Nat. Commun.* **2015**, *6*, 8737.
[6] N. Farsad, E. D. Sone, *J. Struc. Biol.* **2012**, *177*, 613.
[7] B. P. Lee, P. B. Messersmith, J. N. Israelachvili, J. H. Waite, *Annu Rev Mater Res.* **2011**, *41*, 99.
[8] S. C. Daubner, T. Le, S. Wang, *Arch Biochem Biophys.* **2011,** *508*, 1.
[9] V. V. Papov, T. V. Diamond, K. Biemann, J. H. Waite, *J. Biol. Chem.* **1995**, *270*, 20183.
[10] J. H. Waite, X. X. Qin, *Biochemistry* **2001**, *40*, 2887.
[11] J. H. Waite, *J. Exp. Biol.* **2017**, *220*, 517.
[12] N. Bandara, H. Zeng, J. Wu, *J. Adhes. Sci. Technol.* **2013**, *27*, 2139.
[13] J. Zhou, A. P. Defante, F. Lin, Y. Xu, J. Yu, Y. Gao, E. Childers, A. Dhinojwala, M. L. Becker, *Biomacromolecules* **2015**, *16*, 266.
[14] L. Han, Z. -M. Wang, X. Lu, L. Dong, C. -M. Xie, K. -F. Wang, X. -L. Chen, Y. -H. Ding, L. -T. Weng, *Colloids Surf. B* **2015**, *126*, 452.
[15] C. E. Brubaker, P. B. Messersmith, *Biomacromolecules* **2011**, *12*, 4326.
[16] M. Brodie, L. Vollenweider, J. L. Murphy, F. Xu, A. Lyman, W. D. Lew, B. P. Lee, *Biomed. Mater.* **2011**, *6*, 15014.
[17] D. G. Barrett, G. G. Bushnell, P. B. Messersmith, *Adv. Healthcare Mater.* **2013**, *2*, 745.
[18] J. Guo, G. B. Kim, D. Shan, J. P. Kim, J. Hu, W. Wang, F. G. Hamad, G. Qian, E. B. Rizk, J. Yang, *Biomaterials* **2017**, *112*, 275.
[19] M. Mehdizadeh, H. Weng, D. Gyawali, L. Tang, J. Yang, *Biomaterials* **2012**, *33*, 7972.
[20] J. Guo, W. Wang, J. Hu, D. Xie, E. Gerhard, M. Nisic, D. Shan, G. Qian, S. Zheng, J. Yang, *Biomaterials* **2016**, *85*, 204.
[21] K. Huang, B. P. Lee, D. R. Ingram, P. B. Messersmith, *Biomacromolecules* **2002**, *3*, 397.
[22] L. Haeshin, S. M. Dellatore, W. M. Miller, P. B. Messersmith, *Science* **2007**, *318*, 426.
[23] a) P. K. Forooshani, B. P. Lee, *J. Polym. Sci. A* **2017**, *55*, 9; b) M. Krogsgaard, V. Nue, H. Birkedal, *Chem. Eur. J.* **2016**, *22*, 844; c) S. Moulay, *Polymer Reviews* **2014**, *54*, 436; d) J. Sedo, J. Saiz-Poseu, F. Busqué, D. Ruiz-Molina, *Adv. Mater.* **2013**, *25*, 653; e) E. Faure, C. Falentin-Daudre, C. Jerome, J. Lyskawa, D. Fournier, P. Woisel, C. Detrembleur, *Prog. Polym. Sci.* **2013**, *38*, 236; f) B. P. Lee, P. B. Messersmith, J. N. Israelachvili, J. H. Waite, *Annu. Rev. Mater. Res.* **2011**, *41*, 99; g) Q. Ye, F. Zhou, W. Liu, *Chem. Soc. Rev.* **2011**, *40*, 4244.
[24] M. Guardingo, E. Bellido, R. Miralles-Llumà, J. Faraudo, J. Sedó, S. Tatay, A. Verdaguer, F. Busqué, D. Ruiz-Molina, *Small* **2014**, *10*, 1594.
[25] W. Wei , L. Petrone , Y. Tan , H. Cai , J. N. Israelachvili , A. Miserez , J. H. Waite, *Adv. Funct. Mater.* **2016**, *26*, 3496.
[26] S. A. Mian, L. C. Saha, J. Jang, L. Wang, X. Gao, S. Nagase, *J. Phys. Chem. C* **2010**, *114*, 20793.
[27] A. J. Kinloch, *J. Mater. Sci.* **1980**, *15*, 2141.
[28] S. A. Mian, Y. Khan, U. Ahmad, M. A. Khan, G. Rahmanc, S. Ali, *RCS Adv.* **2016**, *6*, 114313.
[29] S. A. Mian, L. -M. Yang, L. C. Saha, E. Ahmed, M. Ajmal, E. Ganz, *Langmuir* **2014**, *30*, 6906.
[30] S. A. Mian, X. Gao, S. Nagase, J. Jang, *Theor. Chem. Acc.* **2011**, *130*, 333.
[31] D. S. Hwang, M. J. Harrington, Q. Lu, A. Masic, H. Zeng, J. H. Waite, *J. Mater. Chem.* **2012**, *22*, 15530.
[32] P. C. Redfern, P. Zapol, L. A. Curtiss, T. Rajh, M. C. Thurnauer, *J. Phys. Chem. B* **2003**, *107*, 11419.
[33] M. Vega-Arroyoa, P. R. LeBretona, T. Rajhb,P. Zapol, L. A. Curtiss, *Chem. Phys. Lett.* **2005**, *406,* 306.
[34] S. -C. Li, J. -G. Wang, P. Jacobson, X. -Q. Gong, A. Selloni, U. Diebold, *J. Am. Chem. Soc.* **2009**, *131*, 980.
[35] M. Benz, K. J. Rosenberg, E. J. Kramer, J. N. Israelachvili, *J. Phys. Chem. B* **2006**, *110*, 11884.

[36] B. Zappone, K. J. Rosenberg, J. N. Israelachvili, *Tribol. Lett.* **2007**, *26*, 191.
[37] F. C. Teng, H. B. Zeng, Q. X. Liu, *J. Phys. Chem. C* **2011**, *115*, 17485.
[38] J. Yu, W. Wei, E. Danner, J. N. Israelachvili, J. H. Waite, *Adv. Mater.* **2011**, *23*, 2362.
[39] U. Terranova, D. R. Bowler, *J. Phys. Chem. C* **2010**, *114*, 6491.
[40] W. M. Chirdon, W. J. O'Brien, R. E. Robertson, *J. Biomed. Mater. Res. B* **2003**, *66B*, 532.
[41] M. B. McBride, L. G. Wesselink, *Environ. Sci. Technol.* **1988**, *22*, 703.
[42] S. L. Simpson, K. J. Powell, S. Sjöberg, *J. Colloid Interface Sci.* **2000**, *229*, 568.
[43] I. -C. Yeh, J. L. Lenhart, B. C. Rinderspacher, *J. Phys. Chem. C* **2015**, *119*, 7721.
[44] L. Yang, S. L. Phua, J. K. H. Teo, C. L. Toh, S. K. Lau, J. Ma, X. Lu, *ACS Appl. Mater. Interfaces* **2011**, *3*, 3026.
[45] S. L. Phua, L. Yang, C. L. Toh, S. huang, Z. Tsakadze, S. K. Lau, Y.-W. Mai, X. Lu, *ACS Appl. Mater. Interfaces* **2012**, *4*, 4571.
[46] S. L. Phua, L. Yang, S. Huang, G. Ding, R. Zhou, J. H. Lew, S. K. Lau, X. Yuan, X. Lu, *Eur. Polym. J.* **2014**, *57*, 11.
[47] C. Leng, Y. Liu, C. Jenkins, H. Meredith, J. J. Wilker, Z. Chen, *Langmuir* **2013**, *29*, 6659.
[48] Z. A. Levine, M. V. Rapp, W. Wei, R. G. Mullen, C. Wu, G. H. Zerze, J. Mittal, J. H. Waite, J. N. Israelachvili, J. -E. Shea, *Proc. Natl. Acad. Sci. U.S.A* **2016**, *113*, 4332.
[49] a) J. Saiz-Poseu, J. Faraudo, A. Figueras, R. Alibes, F. Busqué, D. Ruiz-Molina, *Chem. Eur. J.* **2012**, *18*, 3056; b) J. Saiz-Poseu, I. Alcon, R. Alibes, F. Busqué, J. Faraudo, D. Ruiz-Molina, *CrystEngComm* **2012**, *14*, 264.
[50] X. Wang, Y. Liu, S. Tao, B. Xing, *Carbon* **2010**, *48*, 3721.
[51] C. Wang, S. Li, R. Zhang, Z. Lin, *Nanoscale* **2012**, *4*, 1146.
[52] R. J. Chen, Y. Zhang, D. Wang, H. Dai, *J. Am. Chem. Soc.* **2001**, *123*, 3838.
[53] J. Chen, H. Liu, W. A. Weimer, M. D. Halls, D. H. Waldeck, G. C. Walker, *J. Am. Chem. Soc.* **2002**, *124*, 9034.
[54] J. Björk, F. Hanke, C. -A. Palma, P. Samori, M. Cecchini, M. Persson, *J. Phys. Chem. Lett.* **2010**, *1*, 3407.
[55] H. Hu, M. Chang, M. Zhang, D. Chen, *J. Mater. Sci.* **2017**, *52*, 8650.
[56] F. -f. Liu, J. -l. Fan, S. -g. Wang, G. -h Ma, *Chem. Eng. J.* **2013**, *219*, 450.
[57] D. Lin, B. Xing, *Environ. Sci. Technol.* **2008**, *42*, 7254.
[58] W. Chen, L. Duan, D. Q. Zhu, *Environ. Sci. Technol.* **2007**, *41*, 8295.
[59] X. Sun, H. Shao, K. Xiang, Y. Yan, X. Yu, D. Li, W. Wu, L. Zhou, K. -Fai So, Y. Ren, S. Ramakrishna, A. Li, L. He, *Carbon* **2017**, *113*, 176.
[60] H. Kim, K. H. Ahn, S. J. Lee, *Polymer* **2017**, *110*, 187.
[61] J. Saiz-Poseu, J. Sedó, B. García, C. Benaiges, T. Parella, R. Alibés, J. Hernando, F. Busqué, D. Ruiz-Molina, *Adv. Mater.* **2013**, *25*, 2066.
[62] J. C. Ma, D. A. Dougherty, *Chem. Rev.* **1997**, *97*, 1303.
[63] U. Diebold, *Surf. Sci. Rep.* **2003**, *48*, 53.
[64] R. Sánchez-de-Armas, M. A. San-Miguel, J. Oviedo, A. Márquez, J. F. Sanz, *Phys. Chem. Chem. Phys.* **2011**, *13*, 1506.
[65] S. -C. Li, L. -N. Chu, X. -Q. G, U. Diebold, *Science* **2010**, *328*, 882.
[66] K. L. Syres, A. G. Thomas, W. R. Flavell, B. F. Spencer, F. Bondino, M. Malvestuto, A. Preobrajenski, M. Grätzel, *J. Phys. Chem. C* **2012**, *116*, 23515.
[67] M. J. Jackman, K. L. Syres, D. J. H. Cant, S. J. O. Hardman, A. G. Thomas, *Langmuir* **2014**, *30*, 8761.
[68] K. Syres, A. Thomas, F. Bondino, M. Malvestuto, M. Grätzel, *Langmuir* **2010**, *26*, 14548.
[69] T. D. Savić, M. I. Čomor, J. M. Nedeljković, D. Ž. Veljković, S. D. Zarić, V. M. Rakićc, I. A. Janković, *Phys. Chem. Chem. Phys.* **2014**, *16*, 20796.
[70] J. L. Dalsin, L. Lin, S. Tosatti, J. Vörös, M. Textor, P. B. Messersmith, *Langmuir* **2005**, *21*, 640.
[71] M. Rodenstein, S. Zürcher, S. G. P. Tosatti N. D. Spencer, *Langmuir* **2010**, *26*, 16211.
[72] A. Vittadini, A. Selloni , F. P. Rotzinger , M. Grätzel, *J. Phys. Chem. B* **2000**, *104*, 1300.
[73] H. H. Kristoffersen, J. -E. Shea, H. Metiu, *J. Phys. Chem. Lett.* **2015**, *12*, 2277.
[74] T. Zhang, P. Wojtal, O. Rubela, I. Zhitomirsky, *RSC Adv.* **2015**, *5*, 106877.
[75] W. Lin, J. Walter, A. Burger, H. Maid, A. Hirsch, W. Peukert, D. Segets, *Chem. Mater.* **2015**, *27*, 358.
[76] H. Lee, N. F. Scherer, P. B. Messersmith, *Proc. Natl. Acad. Sci. U.S.A.* **2006**, *103*, 12999.
[77] A. S. Kumar, S. Sornambikai, P. Gayathri, J. -M. Zen, *J. Electroanal. Chem.* **2010**, *641*, 131.
[78] a) M. Oroujeni, B. Kaboudin, W. Xia, P. Jönsson, D. A. Ossipov, *Prog. Org. Coat* .**2018**, *114*, 154; b) C. -Y. Liu, C. -J. Huang, *Langmuir* **2016**, *32*, 5019; c) Y. Liu, K. Ai, L. Lu, *Chem. Rev.* **2014**, *114*, 5057; d) J. Cui, Y. Yan, G. K. Such, K. Liang, C. J. Ochs, A. Postma, F. Caruso, *Biomacromolecules* **2012**, *13*, 2225.
[79] S. Suárez-García, J. Sedó, J. Saiz-Poseu, D. Ruiz-Molina, *Biomimetics* **2017**, *2*, 22.
[80] a) Y. J. Xu, K. Wei, P. Zhao, Q. Feng, C. K. K. Choi, L. Bian, *Biomater. Sci.* **2016**, *4*, 1726; b) D. R. Miller, J. E. Spahn, J. H. Waite, *J. R. Soc. Interface* **2015**, 12: 20150614.
[81] L. M. McDowell, L. A. Burzio, J. H. Waite, J. Schaefer, *J. Biol. Chem.* **1999**, *274*, 20293.
[82] L. Li, H. Zeng, *Biotribology* **2016**, *5*, 44.
[83] J. H. Waite, *Integr. Comp. Biol.* **2002**, *42*, 1172.
[84] L. M. Rzepecki, K. M. Hansen, H. J. Waite, *Biol. Bull.* **1992**, *183*, 123.
[85] C. R. Matos-Pérez, J. J. Wilker, *Macromolecules* **2012**, *45*, 6634.
[86] C. R. Matos-Pérez, J. D. White, J. J. Wilker, *J. Am. Chem. Soc.* **2012**, *134*, 9498.
[87] M. Jia, A. Li, Y. Mua, W. Jiang, X. Wan, *Polymer* **2014**, *55*, 1160.
[88] C. L. Jenkins, H. M. Siebert, J. J. Wilker, *Macromolecules* **2017**, *50*, 561.
[89] M. Ye, R. Jiang, J. Zhao, J. Zhang, X. Yuan, X. Yuan, *Mater Sci: Mater Med* **2015**, *26*, 273.
[90] J. Yang, J. Keijsersa, M. van Heek, A. Stuiver, M. A. Cohen Stuart, M. Kamperman, *Polym. Chem.* **2015**, *6*, 3121.
[91] A. Li, M. Jia, Y. Mu, W. Jiang, X. Wan, *Macromol. Chem. Phys.* **2014**, *216*, 450.
[92] L. Li, Y. Li, X. F. Luo, J. P. Deng, W. T. Yang, *React. Funct. Polym.* **2010**, *70*, 938.
[93] K. Sarbjit, G. M. Weerasekare, R. J. Stewart, *ACS Appl. Mater. Interfaces* **2011**, *3*, 941.
[94] P. Glass, H. Y. Chung, N. R. Washburn, M. Sitti, *Langmuir* **2009**, *25*, 6607.
[95] C. L. Gao, G. Z. Li, H. Xue, W. Yang, F. B. Zhang, S. Y. Jiang, *Biomaterials* **2010**, *31*, 1486.
[96] H. Y. Chung, P. Glass, J. M. Pothen, M. Sitti, N. R. Washburn, *Biomacromolecules* **2011**, *12*, 342.
[97] B. Malisova, S. Tosatti, M. Textor, K. Gademann, S. Zurcher, *Langmuir* **2010**, *26*, 4018.
[98] S. Yuan, D. Wan, B. Liang, S. O. Pehkonen, Y. P. Ting, K. G. Neoh, E. T. Kang, *Langmuir* **2011**, *27*, 2761.
[99] K. H. Bae, Y. B. Kim, Y. Lee, J. Hwang, H. Park, T. G. Park, *Bioconjugate Chem.* **2010**, *21*, 505.
[100] C. L. Jenkins, H. J. Meredith, J. J. Wilker, *ACS Appl. Mater. Interfaces* **2013**, *5*, 5091.
[101] M. Yu, T. J. Deming, *Macromolecules* **1998**, *31*, 4739.
[102] J. Wang, C. Liu, X. Lu, M. Yin, *Biomaterials* **2007**, *28*, 3456.
[103] S. Saxer, C. Portmann, S. Tosatti, K. Gademann, S. Zurcher, M. Textor, *Macromolecules* **2010**, *43*, 1050.
[104] J. V. Alegre-Requena, M. Häring, R. P. Herrera, D. Díaz-Díaz, *New J. Chem.* **2016**, *40*, 8493.
[105] J. Xu, S. Strandman, J. X. X. Zhu, J. Barralet, M. Cerruti, *Biomaterials* **2015**, *37*, 395.
[106] F. Dai, F. Chen, T. Wang, S. Feng, C. Hu, X. Wang, Z. Zheng, *J. Mater. Sci.* **2016**, *51*, 4320.

[107] H. Wu, V. Sariola, J. Zhao, H. Ding, M. Sitti, C. J. Bettinger, *Polym. Int.* **2016**, *65*, 1355.
[108] M. E. R. Shanahan, A. Carre, *Langmuir* **1995**, *11*, 1396.
[109] L. E. Nielsen, R. F. Landel, *Mechanical Properties of Polymers and Composites* **1994**.
[110] S. Seo, S. Das, P. J. Zalicki, R. Mirshafian, C. D. Eisenbach, J. N. Israelachvili, J. H. Waite, B. K. Ahn, *J. Am. Chem. Soc.* **2015**, *137*, 9214.
[111] J. D. White, J. J. Wilker, *Macromolecules* **2011**, *44*, 5085.
[112] D. Lu, Y. Zhang, T. Li, Y. Li, H. Wang, Z. Shen, Q. Wei, Z. Lei, *Polym. Chem.* **2016**, *7*, 1963.
[113] G. P. Maier, M. V. Rapp, J. H. Waite, J. N. Israelachvili, A. Butler, *Science* **2015**, *349*, 628.
[114] C. Lim, J. Huang, S. Kim, H. Lee, H. Zeng, D. S. Hwang, *Angew. Chem. Int. Ed.* **2016**, *55*, 3342.
[115] Y. Li, T. Wang, L. Xia, L. Wang, M. Qin, Y. Li, W. Wang, Y. Cao, *Journal of Materials Chemistry B* **2017,** *5*, 4416.
[116] R. Wang, J. Li, W. Chen, T. Xu, S. Yun, Z. Xu, Z. Xu, T. Sato, B. Chi, H. Xu, *Adv. Funct. Mater.* **2017**, *27*, 1604894.
[117] M. V. Rapp, G. P. Maier, H. A. Dobbs, N. J. Higdon J. H. Waite, A. Butler J. N. Israelachvili, *J. Am. Chem. Soc.* **2016**, *138*, 9013.
[118] B. P. Lee, C. -Y. Chao, F. N. Nunalee, E. Motan, K. R. Shull, P. B. Messersmith, *Macromolecules* **2006**, *39*, 1740.
[119] A. Li, Y. Mu, W. Jiang, X. Wan, *Chem. Commun.* **2015**, *51*, 9117.
[120] M. Brodie, L. Vollenweider, J. L. Murphy, F. Xu, A. Lyman, W. D. Lew, B. P. Lee, *Biomed. Mater.* **2011**, *6*, O015014.
[121] W. Wei, J. Yu, C. Broomell, J. N. Israelachvili, J. H. Waite, *J. Am. Chem. Soc.* **2013**, *135*, 377.
[122] J. Yang, M. A. Cohen Stuart, M. Kamperman, *Chem. Soc. Rev.* **2014**, *43*, 8271.
[123] J. Wu, L. Zhang, Y. Wang Y. Long, H. Gao, X. Zhang, N. Zhao, Y. Cai, J. Xu, *Langmuir* **2011**, *27*, 13684.
[124] K. V. Pillai, S. Renneckar, *Biomacromolecules* **2009**, *10*, 798.
[125] a) M. A. Gebbie, W. Wei, A. M. Schrader, T. R. Cristiani, H. A. Dobbs, M. Idso, B. F. Chmelka, J. H. Waite, J. N. Israelachvili, *Nature Chem.* **2017**, *9*, 473; b) S. Das, N. R. Martinez-Rodriguez, W. Wei, J. H. Waite, J. N. Israelachvili, *Adv. Funct. Mater* **2015**, *25*, 5840.
[126] a) S. Kim, A. Faghihnejad, Y. Lee, Y. Jho, H. Zeng, D. S. Hwang, *J. Mater. Chem. B* **2015**, *3*, 738; b) W. Wei, J. Yu, M. A. Gebbie, Y. Tan, N. R. Martinez-Rodriguez, J. N. Israelachvili, J. H. Waite, *Langmuir* **2015**, *31*, 1105; c) D. S. Hwang, H. Zeng, Q. Lu, J. Israelachvili, J. H. Waite, *Soft Matter.* **2012**, *8*, 5640.
[127] S. Kim, A. Faghihnejad, Y. Lee, Y. S. Jho, H. Zeng, D. S. Hwang, *J. Mater. Chem. B* **2015**, *3*, 738.
[128] J. Yu, W. Wei, E. Danner, R. K. Ashley, J. N. Israelachvili, J. H. Waite , *Nat. Chem. Biol.* **2011**, *7*, 588.
[129] B. J. Sparks, E. F. T. Hoff, L. P. Hayes, D. L. Patton, *Chem. Mater.* **2012**, *24*, 3633.
[130] M. Cencer, M. Murley, Y. Liu, B. P. Lee, *Biomacromolecules* **2015**, *16*, 404.
[131] J. Yang, M. A. C. Stuart, M. Kamperman, *Chem. Soc. Rev*. **2014**, *43*, 8271.
[132] P. Z. Araujo, P. J. Morando, M. A. Blesa, *Langmuir* **2005**, *21*, 3470.
[133] P. Das, M. Reches, *Nanoscale* **2016**, *8*, 15309.
[134] J. Yu, W. Wei, M. S. Menyo, A. Masic, J. H. Waite, J. N. Israelachvili, *Biomacromolecules* **2013**, *14*, 1072.
[135] M. Cencer, Y. Liu, A. Winter, M. Murley, H. Meng, B. P. Lee, *Biomacromolecules* **2014**, *15*, 2861.
[136] Y. Kan, E. W. Danner, J. N. Israelachvili, Y. Chen, J. H. Waite, *PLoS One* **2014**, *9 (10)*, e108869.
[137] A. R. Narkar, B. Barker, M. Clisch, J. Jiang, B. P. Lee *Chem. Mater*. **2016**, *28*, 5432.
[138] J. Lee, K. C. Yoo, J. Ko, B. Yoo, J. Shin, S. J. Lee, D. Sohn, *Carbohydrate Polymers* **2017**, *164*, 309.
[139] C. A. Del Grosso, T. W. McCarthy, C. L. Clark, J. L. Cloud, J. J. Wilker, *Chem. Mater*. **2016**, *28*, 6791.
[140] J. Monahan, J. J. Wilker, *Chem. Commun.* **2003**, 1672.
[141] J. J. Wilker, *Angewandte Chem. Int. Ed*. **2010**, *49*, 8076.
[142] S. W. Taylor, J. H. Waite, M. M. Ross, J. Shabanowitz, D. F. Hunt, *J. Am. Chem. Soc*. **1994**, *116*, 10803.
[143] a) S. G. George, B. J. S. Pirie, T. L. Coombs, *J. Exp. Mar. Biol*. **1976**, *23*, 71; b) T. L. Coombs, P. J. Keller, *Aquat. Toxicol*. **1981**, *1*, 291.
[144] J. R. Donat, K. W. Bruland In Trace Elements in Natural Waters; Salbu, B., Steinnes, E., Eds.; CRC Press: Ann Arbor, MI, **1995**; 247.
[145] D. E. Fullenkamp, D. G. Barrett, D. R. Miller, J. W. Kurutz, P. B. Messersmith, *RSC Adv*. **2014**, *4*, 25127.
[146] N. Holten-Andersen, M. J. Harrington, H. Birkedal, B. P. Lee, P. B. Messersmith, K. Y. C. Lee, J. H. Waite, *Proc. Natl. Acad. Sci.* **2011**, *108*, 2651.
[147] H. Zeng, D. S. Hwang, J. N. Israelachvili, J. H. Waite, *Proc. Natl. Acad. Sci*. **2010**, *107*, 12850.
[148] a) D. J. Rubin, A. Miserez, J. H. Waite, *Advances in Insect Physiology*, Vol. 38; b) C. Jérôme, J. S. Stephen Eds.; *Academic Press: London*, *2010*; Chapter 3, pp 75-133; c) E. Degtyar, M. J. Harrington, Y. Politi, P. Fratzl, *Angew. Chem., Int. Ed*. **2014**, *53*, 12026.
[149] M. J. Harrington, A. Masic, N. Holten-Andersen, J. H. Waite, P. Fratzl, *Science*, **2010**, *328*, 216.
[150] Fan Zhang, Majid Sababi, Tore Brinck, Dan Persson, Jinshan Pan,, Per M. Claesson, *J. Colloid Int. Sci*. **2013**, *404*, 62.
[151] N. Holten-Andersen, G. E. Fantner, S. Hohlbauch, J. H. Waite, F. W. Zok, *Nat. Mater*. **2007**, *6*, 669.
[152] a) B. J. Kim, S. Kim, D. X. Oh, A. Masic, H. J. Cha, D. S. Hwang, *J. Mater. Chem. B* **2015**, *3*, 112; b) B. J. Kim, H. Cheong, B. H. Hwang, H. J. Cha, *Angew. Chem., Int. Ed*. **2015**, *54*, 7318; c) B. J. Kim, D. X. Oh, S. Kim, J. H. Seo, D. S. Hwang, A. Masic, D. K. Han, H. J. Cha *Biomacromolecules* **2014**, *15*, 1579; d) Q. Li, D. G. Barrett, P. B. Messersmith, N. Holten-Andersen, *ACS Nano* **2016**, *10*, 1317.
[153] N. Holten-Andersen, T. E. Mates, M. S. Toprak, G. D. Stucky, F. W. Zok, J. H. Waite, *Langmuir* **2009**, *25*, 3323.
[154] a) S. Das, D. R. Miller, Y. Kaufman, N. R. Martinez-Rodriguez, A. Pallaoro, M. J. Harrington, M. Gylys, J. N. Israelachvili, J. H. Waite, *Biomacromolecules* **2015**, *16*, 1002; b) S. Das, N. R. M. Rodriguez, W. Wei, J. H. Waite, J. N. Israelachvili, *Adv. Funct. Mater*. **2015**, *25*, 5840.
[155] a) L. A. Burzio, J. H. Waite *Biochemistry* **2000**, *39*, 11147; b) Y. Miaoer, J. W. Hwang, T. J. Deming, *J. Am. Chem. Soc*. **1999**, *121*, 5825.
[156] M. A. Matin, R. K. Chitumalla, M. Lim, X. Gao, J. Jang, *J. Phys. Chem. B* **2015**, *119*, 5496.
[157] B. P. Frank, G. Belfort, *Biotechnol. Prog*. **2002**, *18*, 580.
[158] S. W. Taylor, D. B. Chase, M. H. Emptage, M. J. Nelson, J. H. Waite, *Inorg. Chem*. **1996**, *35*, 7572.
[159] S. W. Taylor, G. W. Luther, J. H. Waite, *Inorg. Chem*. **1994**, *33*, 5819.
[160] H. Ceylan, M. Urel, T. S. Erkal, A. B. Tekinay, A. Dana, M. O. Guler, *Adv. Funct. Mater*. **2013**, *23*, 2081.
[161] M. J. Sever, J. T. Weisser, J. Monahan, S. Srinivasan, J. J. Wilker, *Angew. Chem., Int. Ed*. **2004**, *43*, 448.
[162] B. Yang, C. Lim, D. S. Hwang, H. J. Cha, *Chem. Mater*. **2016**, *28*, 7982.
[163] G. P. Maier, A. Butler, *J. Biol. Inorg. Chem*. **2017**, *22*, 739.
[164] J. J Wilker, *Current Opinion in Chemical Biology* **2010**, *14*, 276.
[165] H. Ejima, J. J. Richardson, F. Caruso, *Nano Today* **2017**, *12*, 136.
[166] Q. Wei, K. Achazi, H. Liebe, A. Schulz, P.-L. M. Noeske, I. Grunwald, R. Haag, *Angew. Chem. Int. Ed*. **2014**, *53*, 11650.
[167] B. P. Lee, S.i Konst, *Adv. Mater*. **2014**, *26*, 3415.
[168] S. Hou, P.r X. Ma, *Chem. Mater*. **2015**, *27*, 7627.
[169] J. Hedlund, M. Andersson, C. Fant, R. Bitton, H. Bianco-Peled, H. Elwing, M. Berglin, *Biomacromolecules* **2009**, *10*, 845.
[170] C. Fant, K. Sott, H. Elwing, F. Hook, *Biofouling* **2000**, *16*, 119.

[171] C. N. Schmitt, A. Winter, L. Bertinetti, A. Masic, P. Strauch, M. J. Harrington, *J. R. Soc. Interface*. **2015**, 12(110):0466.
[172] J. Monahan, J. J. Wilker, *Langmuir* **2004**, *20*, 3724.
[173] L. Yang, J. Kong, D. Zhou, J. M. Ang, S. L. Phua, W. A. Yee, H. Liu, Y. Huang, X. Lu, *Chem. Eur. J*. **2014**, *20*, 7776.

REVIEW

A suitable chemical toolbox to understand the different parameters, both inherent to the polymer backbone and external (such as pH or the presence of metal ions), influencing the adhesion and cohesion of catechol-based coatings and adhesives is given.

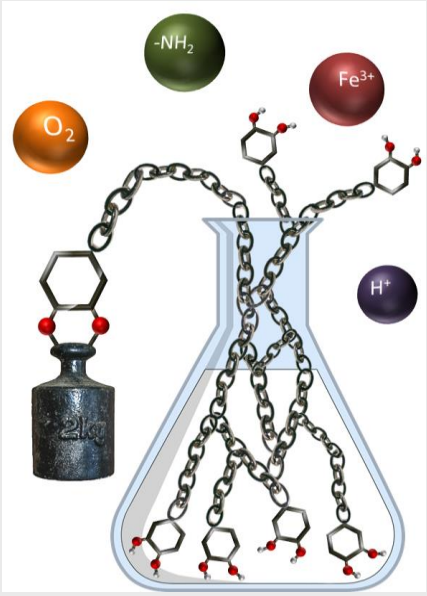

J. Saiz-Poseu, J. Mancebo-Aracil, F. Nador, F. Busqué, D. Ruiz-Molina**

Page No. – Page No.

The Chemistry behind Catechol-Based Adhesion